

**CHARACTERIZATION AND PURIFICATION OF
WASTEWATER SLUDGE FROM RUBBER
INDUSTRY FOR VALUE-ADDED APPLICATION**

TAN XUAN LER

UNIVERSITI TUNKU ABDUL RAHMAN

**CHARACTERIZATION AND PURIFICATION OF WASTEWATER
SLUDGE FROM RUBBER INDUSTRY FOR VALUE-ADDED
APPLICATION**

TAN XUAN LER

**A project report submitted in partial fulfilment of the
requirements for the award of Bachelor of Chemical
Engineering with Honours**

**Lee Kong Chian Faculty of Engineering and Science
Universiti Tunku Abdul Rahman**

April 2024

DECLARATION

I hereby declare that this project report is based on my original work except for citations and quotations which have been duly acknowledged. I also declare that it has not been previously and concurrently submitted for any other degree or award at UTAR or other institutions.

Signature : *xuanler*

Name : Tan Xuan Ler

ID No. : 1902901

Date : 18 April 2024

APPROVAL FOR SUBMISSION

I certify that this project report entitled “**CHARACTERIZATION AND PURIFICATION OF WASTEWATER SLUDGE FROM RUBBER INDUSTRY FOR VALUE-ADDED APPICATION**” was prepared by **TAN XUAN LER** has met the required standard for submission in partial fulfilment of the requirements for the award of Bachelor of Chemical Engineering with Honours at Universiti Tunku Abdul Rahman.

Approved by,

Signature : *steven*

Supervisor : Dr. Steven Lim

Date : 26 April 2024

The copyright of this report belongs to the author under the terms of the copyright Act 1987 as qualified by Intellectual Property Policy of Universiti Tunku Abdul Rahman. Due acknowledgement shall always be made of the use of any material contained in, or derived from, this report.

© 2024, Tan Xuan Ler. All right reserved.

ACKNOWLEDGEMENTS

In completing for this research project, I have been fortunate to receive support, inspiration and guidance of many individuals. Firstly, I would like to extend my sincere thanks to my esteemed supervisor, Dr Steven Lim, for his invaluable guidance, feedback and mentorship throughout this project. His patience and dedication have inspired me to strive for greatness.

Moreover, I am grateful to the staff of Universiti Tunku Abdul Rahman (UTAR), at Lee Kong Chian Faculty of Engineering and Science (LKC FES), for providing access to resources, research materials and facilities. The conducive academic environment greatly facilitated the experimental work and analysis conducted as part of this project.

Furthermore, special appreciation goes to the postgraduate students, Mr. Lee Sean Jun and Mr. Chai Kian Hoong, who generously contributed their time, advice and insights in operating the instruments. Besides, I would like to thank my family for their constant encouragement throughout my academic journey. Last but not least, I am grateful to my friends and coursemates for their moral support and assistance in the completion of this study.

ABSTRACT

Rubber industries in Malaysia generate substantial volume of wastewater, ranging from 50 to 55 thousand m³ during raw rubber production and 100 to 130 thousand m³ daily for its derivatives manufacturing. Treating this wastewater has generated 240 tons of sludge annually. Due to the ineffective sludge management plan, the sludge is underutilized. A novel process that converts this sludge into valuable compound, while minimizing final waste would be a promising solution in the treatment of sludge. The composition of sludge from the rubber industry is highly complex due to various chemicals introduced during the manufacturing process, posing challenges to treatment. In this study, various characterization methods, including FTIR, SEM-EDX, XRD and TGA were conducted to provide insights into sludge properties. Along with that, Ca and Al were found to be the major components. Subsequently, an Aqua Regia digestion method was employed to determine the total metal concentration within the sludge. The concentration of Ca was found to be 71.88 mg/g of sludge, whereas the concentration of Al was found to be 47.47 mg/g of sludge. To treat the sludge and extract these prominent metals, acid leaching was selected as the treatment method. The leaching efficiency was investigated by adjusting its parameters: acid selection (H₂SO₄, HNO₃, HCl), molar concentration of the acid (0.3, 0.5 and 1.0 M), liquid-to-solid ratio (3:1, 5:1 and 10:1), temperature (30, 50, 70 and 90 °C), as well as duration (30, 60, 90 and 120 minutes). In this context, using 1.0 M HNO₃ at a liquid-to-solid ratio of 10:1, under 90 °C for 90 minutes were determined as the optimum conditions for the acid leaching treatment process for the rubber sludge. The Al extraction efficiency achieved 100 %, while Ca reached 95.21 %. Further analysis of the post-leached residues indicated their potential for reuse as low-cost adsorbents, soil conditioners or energy sources. Not only that, but the Al and Ca in leachate could be recovered and utilized in other applications.

TABLE OF CONTENTS

DECLARATION		i
APPROVAL FOR SUBMISSION		ii
ACKNOWLEDGEMENTS		iv
ABSTRACT		v
TABLE OF CONTENTS		vi
LIST OF TABLES		ix
LIST OF FIGURES		x
LIST OF SYMBOLS / ABBREVIATIONS		xii
LIST OF APPENDICES		xiv
CHAPTER		
1	INTRODUCTION	1
1.1	Wastewater Generation from Rubber Production	1
1.2	Sludge Generation	3
1.3	Problem Statement	4
1.4	Significance of the Study	6
1.5	Aim and Objectives	7
1.6	Scope and Limitations of the Study	7
1.7	Outline of the Report	8
2	LITERATURE REVIEW	9
2.1	Introduction	9
2.2	Sludge Management	9
2.2.1	Moisture Removal	9
2.2.2	Lime Stabilization	13
2.2.3	Aerobic Digestion	13
2.2.4	Anaerobic Digestion	13
2.3	Characterization Study of Sludge	15
2.3.1	Fourier-Transform Infrared Spectroscopy (FTIR)	15

2.3.2	Scanning Electron Microscopy-Energy Dispersive X-Ray (SEM-EDX)	17
2.3.3	X-ray Diffraction (XRD)	19
2.3.4	Thermogravimetric Analysis (TGA)	20
2.4	Sludge Digestion Study	22
2.4.1	Single Acid Digestion	22
2.4.2	Acid Mixtures Digestion	23
2.5	Metal Removal from Sludge	24
2.5.1	Acid Leaching	25
2.5.2	Effect of Acid on Leaching Rate	26
2.5.3	Effect of Time on Leaching Rate	26
2.5.4	Effect of Temperature on Leaching Rate	27
2.5.5	Effect of Acid Concentration on Leaching Rate	29
2.5.6	Effect of Liquid-to-Solid Ratio on Leaching Rate	30
2.5.7	Optimum Combination of the Factors	31
2.6	Hydrocarbon Recovery	34
2.6.1	Solvent Extraction Method	34
2.6.2	Effect of Solvent on Removal Efficiency	34
2.6.3	Effect of Duration on Removal Efficiency	35
2.6.4	Effect of Solvent-to-Sludge ratio on Removal Efficiency	35
2.6.5	Optimum Combination of the Factors	36
3	METHODOLOGY AND WORK PLAN	38
3.1	List of Materials and Equipment	38
3.1.1	Materials and Chemicals	38
3.1.2	Equipment and Apparatus	38
3.2	Overall Flowchart	39
3.3	Pre-Treatment of Sludge	40
3.4	Characterization Study of Sludge	41
3.4.1	FTIR	41
3.4.2	SEM-EDX	41
3.4.3	XRD	41

3.4.4	TGA	42
3.5	Sludge Digestion	42
3.6	Treatment of Sludge	42
3.7	Sample Analysis	44
4	RESULTS AND DISCUSSION	45
4.1	Characterization Study of Raw Sludge	45
4.1.1	FTIR	45
4.1.2	SEM-EDX	47
4.1.3	XRD	50
4.1.4	TGA	52
4.2	Acid Digestion of Sludge	53
4.3	Parameter Studies in Acid Leaching of Sludge	54
4.3.1	Effect of Types of Acids and its Concentration	54
4.3.2	Effect of Liquid-to-Solid Ratio	56
4.3.3	Effect of Temperature	58
4.3.4	Effect of Duration	59
4.4	Post-Leached Residues Studies	60
4.4.1	Physical Appearances	60
4.4.2	SEM	61
4.4.3	FTIR	62
4.4.4	XRD	64
4.5	Potential for Reutilization	65
5	CONCLUSIONS AND RECOMMENDATIONS	67
5.1	Conclusions	67
5.2	Recommendations for Future Work	68
	REFERENCES	70
	APPENDICES	82

LIST OF TABLES

Table 2.1:	Types of Water in Sludge with its Removal Process Processing (Dichtl and Kopp, 2000; Novak, 2006; Kamizela and Kowalczyk, 2019).	10
Table 2.2:	Comparative Analysis of Sludge Moisture Removal Processes.	11
Table 2.3:	Functional Groups in CLS.	15
Table 2.4:	Elemental Analysis for Rubber Wastes.	18
Table 2.5:	Advantages and Disadvantages of Technologies in Heavy Metals Removal from Sludge (Geng, et al., 2020; Soliman and Moustafa, 2020).	25
Table 2.6:	Leaching Efficiency over Time.	27
Table 2.7:	Comparison of Metals Removal Efficiency.	32
Table 2.8:	Comparison of Oil Recovery Efficiency using Solvent Extraction.	37
Table 3.1:	Chemicals Used in the Experiment.	38
Table 3.2:	Apparatus and Equipment Used in the Experiment.	39
Table 4.1:	Elemental Composition of Sludge from EDX.	49

LIST OF FIGURES

Figure 1.1:	Raw Natural Rubber Processing Process (Devaraj, Zairossani and Pretibaa, 2006; Gamaralalage, Sawai and Nunoura, 2016).	2
Figure 1.2:	Sludge Generation Through Wastewater Treatment Operation (Laura Martín-Pozo, et al., 2022).	3
Figure 1.3:	Trend of Waste Output under Code SW 321 (Department of Environment, 2022).	5
Figure 2.1:	Water Distribution Inside the Sludge (Guangyin and Youcai, 2017).	10
Figure 2.2:	Simplified Diagram of Anaerobic Digestion (Dentel and Qi, 2013).	14
Figure 2.3:	FTIR Spectrum of Natural Rubber (Rolere, et al., 2015).	16
Figure 2.4:	Chemical Structure of Isoprene (Ali Fazli and Rodrigue, 2020).	17
Figure 2.5:	SEM Images of (a) Recycled Rubber Waste (Abbas, et al., 2022), (b) Raw Rubber Crumb (Haworth, et al., 2018) and (c) Crushed Rubber Crumb (Bisht and Ramana, 2017).	18
Figure 2.6:	XRD Pattern of Rubber Sludge (Uttara Mahapatra, Ajay Kumar Manna and Abhijit Chatterjee, 2022).	20
Figure 2.7:	XRD Pattern of Raw Rubber Crumb (Roychand, et al., 2021).	20
Figure 2.8:	TGA under Nitrogen or Air (Uttara Mahapatra, et al., 2021).	21
Figure 2.9:	Leaching Efficiency of Al Under Different Temperature.	29
Figure 2.10:	Leaching Efficiency of (a) Ni, (b) Cu, (c) Cr and (d) Pb.	30
Figure 3.1:	Flow Chart of Overall Study.	40
Figure 3.2:	Experimental Setup of Acid Leaching.	43
Figure 4.1:	FTIR Spectrum of Raw Rubber Sludge.	46
Figure 4.2:	SEM Images of Raw Rubber Sludge at Magnification of (a) 500X, (b) 2000X and (C) 5000X.	48

Figure 4.3:	XRD of Raw Rubber Sludge.	51
Figure 4.4:	TGA Curve of Raw Rubber Sludge.	52
Figure 4.5:	Extraction Efficiency using Different Acids and Concentration on (a) Ca and (b) Al.	54
Figure 4.6:	Effect of L/S Ratio on Extraction Efficiency of Ca and Al.	57
Figure 4.7:	Effect of Temperature on Extraction Efficiency of Ca and Al.	58
Figure 4.8:	Effect of Duration on Extraction Efficiency of Ca and Al.	59
Figure 4.9:	Physical Appearance of (a) RAS and (b) ROR.	61
Figure 4.10:	Morphology of the (a) RAS with H ₂ SO ₄ and (b) ROR.	61
Figure 4.11:	FTIR Spectra of RAS with H ₂ SO ₄ and ROR.	63
Figure 4.12:	Diffraction Peaks of RAS with H ₂ SO ₄ and ROR.	64

LIST OF SYMBOLS / ABBREVIATIONS

A	frequency factor
C	leached Ca and Al content, mg/g
C_{total}	total Ca and Al in the solid sample, mg/g
E_a	activation energy
k	rate constant
R	gas constant, 8.314 J/molK
K_d	discharge coefficient
T	temperature, K
Al	aluminium
Al(OH) ₃	gibbsite
Al(NO ₃) ₃ ·9H ₂ O	aluminium nitrate nonahydrate
C	carbon
CaCO ₃	calcium carbonate / calcite
CaMg(CO ₃) ₂	dolomite
Ca(NO ₃) ₂ ·4H ₂ O	calcium nitrate tetrahydrate
CaO	quicklime
CaSO ₄	calcium sulfate
Cl	chlorine
Cr	chromium
Cu	copper
Fe	iron
Fe ₂ O ₃	hematite
H ⁺	hydrogen ions
HCl	hydrochloric acid
HF	hydrofluoric acid
HNO ₃	nitric acid
H ₂ S	hydrogen sulfide
H ₂ SO ₄	sulfuric acid
K	potassium
Mg	magnesium
Na	sodium

N-H	amine group
Ni	nickel
O	oxygen
P	phosphorus
Pb	lead
S	sulfur
Si	silicon
SiO ₂	silica
Zn	zinc
BS	biosludge
CLS	concentrated latex sewage sludge
FAAS	flame atomic absorption spectroscopy
FOG	fats, oils and grease
FTIR	fourier-transform infrared spectroscopy
HHV	higher heating value
ICP-MS	inductively coupled plasma – mass spectrometry
ICP-OES	inductively coupled plasma – optical emission spectrometry
L/S	liquid-to-solid
LPG	liquified petroleum gas
MEK	methyl ethyl ketone
NR	natural rubber
RAS	residues from acid selection studies
ROR	residues from the optimal results
RSS	ribbed smoked sheets
S/S	solvent-to-sludge
SW	Solid Waste
SEM-EDX	scanning electron microscopy – energy dispersive x-ray
SW	solid waste
TGA	thermogravimetric analysis
TSR	technically specified rubber
v/v	volume per volume
WTP	wastewater treatment plant
XRD	x-ray diffraction

LIST OF APPENDICES

Appendix A: Preparation for Multi-Element Standard Solution	82
Appendix B: EDX Result of Residues from Acid Digestion	84
Appendix C: Preparation of Acid for Leaching Process	85
Appendix D: ICP-OES Result Analysis	86
Appendix E: EDX Results of Post-Leached Sludge with HNO ₃	88

CHAPTER 1

INTRODUCTION

1.1 Wastewater Generation from Rubber Production

In the year of 2023, Malaysia had produced approximately 160 thousand tons of natural rubber, securing its position as the seventh largest producer globally. Furthermore, rubber industry's contribution extends to exports, as being the fifth largest exporter worldwide. The extensive growth in the production of natural rubber, encompassing concentrated latex, crepe rubber, technically specified rubber (TSR) and ribbed smoked sheets (RSS), requires a significant volume of water, leading to the generation of substantial effluent from the operations (Dunuwila, et al., 2020; Hasyimah Rosman, et al., 2013).

Figure 1.1 illustrates the stages involved in treating the raw latex to prepare it for a wide range of industrial applications. According to Gamaralalage, Sawai and Nunoura (2016), wastewater generated during manufacturing of concentrated latex primarily arises from the centrifugation process, which necessitates plenty of water for cleaning the rotating blades. In the production of crepe rubber, RSS, and TSR, the effluent predominantly originates from the coagulation, wet-milling, water dipping or post-cleaning processes. Moreover, a significant volume of water serves as the heating or cooling utility throughout the various stages of manufacturing (Massoudinejad, et al., 2015). The statistics indicated that in the course of processing raw natural rubber, 50 to 55 thousand cubic meters of wastewater was generated per day (Devaraj, 2021).

After the natural rubber is processed, it can be used to make various rubber products in industries. For example, concentrated latex serves as the main raw material for manufacturing of gloves, catheters and latex thread, while TSR is mainly for the production of tyres and car components (Devaraj, Zairossani and Pretibaa, 2006). Among these natural rubber products, Malaysia has consistently maintained its dominance in the global glove market over the past few years, accounting for 67 % of the world's supply of rubber gloves (Khoo, 2023). The main sources for wastewater generation in rubber gloves manufacturing line come from former cleaning, coagulant dipping,

latex compounding and dipping, as well as leaching to eliminate residual chemicals from the surface of the gloves. To highlight, the downstream phases of rubber product manufacturing exhibited a notable escalation in wastewater output compared to the raw latex processing stage, reaching a recorded volume ranging between 100 to 130 thousand cubic meters daily (Devaraj, 2021).

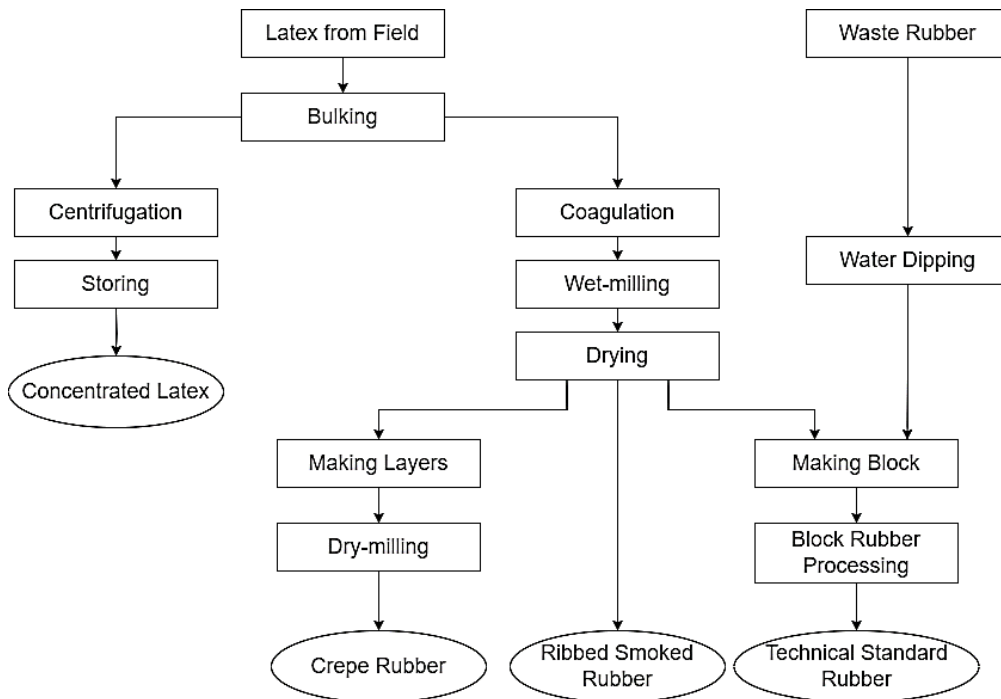


Figure 1.1: Raw Natural Rubber Processing Process (Devaraj, Zairossani and Pretibaa, 2006; Gamaralalage, Sawai and Nunoura, 2016).

On top of that, the daily release of approximately 80 thousand cubic meters of untreated rubber effluent into nearby streams and rivers has been documented in Malaysia. Without proper treatment, the discharge of effluent from the rubber processing industry into the environment could result in severe, hazardous, and long-lasting consequences. Therefore, it is essential to employ suitable technologies and adequate wastewater treatment plants to manage these effluents (Massoudinejad, et al., 2015). Nevertheless, the wastewater treatment operations unavoidably lead to the production of sludge, as it is an inevitable by-product of the process.

1.2 Sludge Generation

In accordance with Water Services Industry Act (2006), sludge refers to the residual mixture of solids and liquids generated during the partial or full wastewater treatment processes, explicitly excluding the treated sewage effluent that is released through a disposal pipe. Such sludge is generally classified as waste, or even hazardous waste (Santos and Lopes, 2022).

Starting from 1970s, industries have been obligated to adhere to stringent environmental legislation such as the Environmental Quality Act 1974 and the Environmental Quality (Sewage) Regulations 2009, which impose compliance with effluent discharge standards. This has prompted the continual expansion of wastewater treatment facilities through the implementation of new installations and upgrades (Academy of Sciences Malaysia, 2015). As a result, there has been a significant increase in the generation of sludge, which predominantly settles during the primary and secondary treatment stages in the clarifiers (Yang, et al., 2020). Figure 1.2 clearly depicts the major steps of the wastewater treatment process, culminating in the formation of sludge.

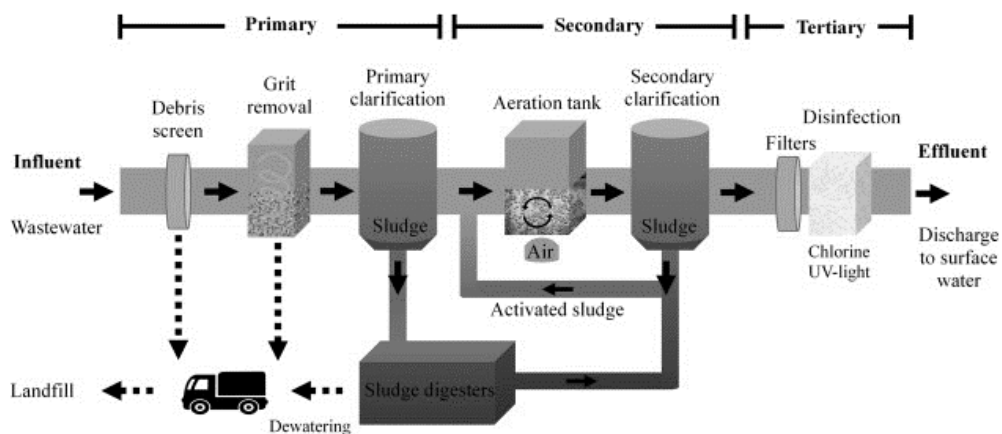


Figure 1.2: Sludge Generation Through Wastewater Treatment Operation
(Laura Martín-Pozo, et al., 2022).

With a large manufacturing rate of natural rubber and its products, it was reported that around 240 tons of sludge from rubber industry were formed annually (Rani, et al., 2020). While many lab-scale studies have experimented with techniques to generate a low sludge yield, sludge generation at the industrial level can still reach up to 10 tons monthly (Wijerathna, et al., 2023).

The composition of the sludge is determined by the pollution load, the nature of the wastewater treated and the methods of treatment employed. Based on Arif Billah, et al. (2020), the sludge is typically composed of a heterogeneous mixture of undigested organic and inorganic compounds. In comparison to municipal sewage sludge, industrial sludge tends to be enriched with higher concentration of dissolved metals. It is due to the substantial quantity of chemicals introduced during the production line and being concentrated in the sludge after wastewater treatment (Devi and Saroha, 2017). This indicates that managing this sludge is likely to become more challenging and problematic.

According to Wijerathna, et al. (2023), the sludge formed during the rubber wastewater treatment operations is often landfilled, incinerated or discharged into agricultural fields without any special treatment. These common practices for disposing of sludge could potentially pose pollution risks to environment and result in health hazards (Arif Billah, et al., 2020). Besides, treating the large volume of sludge involves a considerable share of the total operational expenses of water treatment facilities (Lamastra, et al., 2018). It has been asserted that the overall expenses associated with sludge management and handling may make up to 50 % of the total operational costs of the wastewater treatment plant, despite the fact that the sludge volume to be treated is less than one percent of the total wastewater volume (Nielsen and Stefanakis, 2020). To further highlight, it is anticipated to cost at least another RM 3.1 billion to install adequate treatment facilities by the end of 2035, due to the existing infrastructure for sludge treatment is constrained (Indah Water, 2019).

Therefore, considering both environmental and economic perspectives, the safe disposal and proper reutilization of sludge have become pressing issues. In this context, continuous efforts in the treatment of sludge should be invested, aiming not only to reclaim its valuable components, but also convert this waste into value-added application.

1.3 Problem Statement

The growth of the rubber products manufacturing sector in Malaysia has not only contributed to the substantial economic growth for the country, but it has

also resulted in the generation of a high volume of waste. In this context, rubber industrial wastewater sludge has been officially categorized as schedule waste under the stringent Solid Waste (SW) 321 code. Over the past few years, the quantity of waste generated within this category has exhibited a continuous upward trend, as illustrated in Figure 1.3.

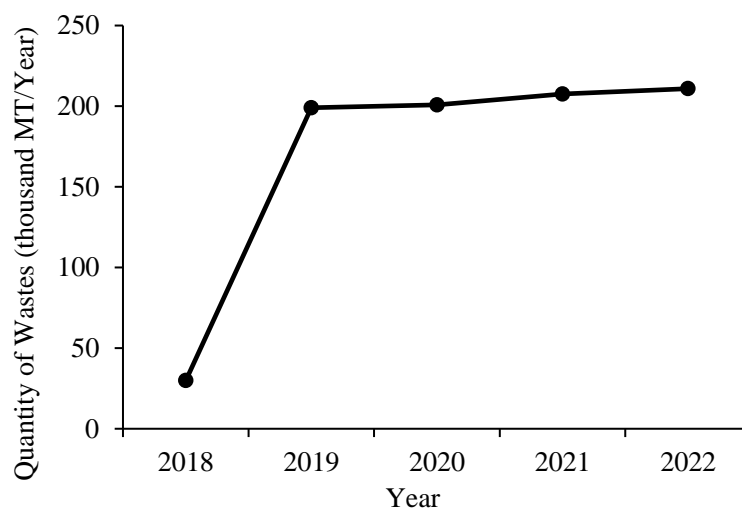


Figure 1.3: Trend of Waste Output under Code SW 321 (Department of Environment, 2022).

As mentioned, the most applied disposal methods for the industrial sludge are landfill, incineration and land application (Noorain, 2013). However, the scarcity of available landfill sites, coupled with concerns about secondary pollution and greenhouse gas emissions, is exerting great pressure on the landfill disposal method. Another approach to adding value to the sludge is through incineration, as it offers the maximum volume reduction for final disposal. However, a limitation of this technique is the formation of toxic combustion by-products, including dioxins and furans, which eventually raised the issues about the potential exposure to hazardous pollutants (Devi and Saroha, 2017).

Sludge land application is recognized as a sustainable approach to sludge management, as industrial sludge comprises organic compounds enriched with nitrogen, phosphorus, and potassium. This composition can significantly enhance soil fertility and support plant growth. Nevertheless, high concentration of inorganic materials, such as heavy metals and other trace

elements in sludge limits its application to land (Yang, et al., 2020). It is mainly due to the reason that these metals are not biodegradable, and the detrimental nature of these substances give rise to environmental risks and threats to human health through the food chain.

In addition, large amount of sludge is being underutilized, which represents an untapped opportunity for the recovery of profitable component, such as metals within the sludge and for the reuse of the sludge itself (Chen, Ma and Dai, 2010). In this regard, with proper treatment, this industrial sludge can be considered as a valuable source to be reused in other applications, while minimizing the final waste. Indeed, the composition of sludge remains complex. This may render challenges in accurately identify the elements present, thereby hindering the selection of the most appropriate treatment method. Therefore, characterizing the physical and chemical properties of sludge to determine the most prominent elements is necessary before the treatment being carried out.

1.4 Significance of the Study

Research into the characterization and appropriate treatment method for sludge can help to address the common public perception of sludge from wastewater treatment plants as mere waste. In fact, all kinds of substances, like organic matter, nutrients, and metals which present in the sludge can be recovered, offering an alternative to the conventional approach of final disposal that leads to numerous environmental, social and economic implications. To further highlight, extracting valuable resources from the sludge contributes to the circular economy. It is mainly due to the fact that the recovered substances can be converted into marketable commodities, whereas the sludge can also be given a second life by fully repurposing it in other field. Furthermore, it has been reported that approximately 25 % of the treatment costs could potentially be saved through resource recovery from sludge (Rakotonimaro, et al., 2017).

However, the predominant focus in existing research lies in addressing the removal of organic matter and reducing pathogen concentration in sludge. Consequently, there is a distinct lack of attention on the effectiveness of methods for removing inorganic matter industrial sludge. To bridge this gap, research interest in this industrial waste revolves around

gaining a deeper understanding of the complex constituents of sludge from the rubber industry. It indirectly allowing for the quantification of essential inorganic substances within it. This knowledge facilitates the development of proper treatment method with optimal parameters to extract these elements, enhancing their potential for recovery and eventual purification of the sludge to be reclaimed and repurposed. It contributes to Sustainable Development Goals 9, 12, and 13 by improving resource use efficiency, promoting sustainable waste management, and reducing hazardous sludge disposal.

1.5 Aim and Objectives

The aim of this research was to study the characteristics of sludge collected from the wastewater treatment plant in rubber industry, identify the most prominent elements present within the sludge and investigate the removal efficiency based on the suggested method.

The objectives of this project include:

1. To determine the physical and chemical characteristics of the sludge from the effluent of rubber industry.
2. To evaluate the effects of the different operating parameters on the removal efficiency of calcium and aluminium through acid leaching.
3. To characterize the post-leached residues in order to determine the potential reutilization.

1.6 Scope and Limitations of the Study

This study covers the analysis of the physical and chemical characteristic of the sludge, including the functional group attached, mineral structure, thermal stability, as well as the surface morphology and elemental analysis.

After identifying the most abundant metal elements, which are calcium and aluminium, the sludge is digested using Aqua Regia to quantify their actual concentration. Therefore, the extraction efficiency can be evaluated in the subsequent steps.

Based on the information about the compounds present, treatment method, which is acid leaching is carried out. Different types of acids are employed to investigate the leaching efficiency of these compounds from the sludge. The operating parameters of leaching process, including temperature,

acid concentration, duration, liquid-to-solid ratio are manipulated to achieve the optimum extraction efficiency. Subsequently, the post-leached residues undergo testing to evaluate the impact of the acid treatment on them.

Several limitations in this study should be acknowledged for future improvements. Firstly, this study focuses solely on the removal of two specific metals, namely aluminium and calcium, which are found in high concentration within the sludge. Organic elements such as the nitrogen, phosphorus and potassium are not considered in this study. Apart from that, the sludge digestion step is conducted only through the Aqua Regia extraction, as the equipment malfunction prevents the incorporation of microwave-assisted total digestion. This limitation may ultimately affect the depth and breadth of the research concerning the initial metal concentration within the sludge. Besides, the study is limited to the use of three different types of inorganic acids, which are hydrochloric acid, nitric acid and sulfuric acid as the extractants in the leaching process.

1.7 Outline of the Report

The report will be specified into five chapters. Chapter 1 provides a general introduction to the topic, focusing on wastewater generation in the rubber industry, and its resulting sludge production. Besides, problem statement, significance of the study, aim and objectives, along with the scope and limitations are included.

Chapter 2 delves into a comprehensive literature review, covering sludge management techniques, characterization analyses specific to waste from the rubber industries, sludge digestion techniques and treatment methods for extracting elements within the sludge.

Chapter 3 highlights the research methodology and experiment planning, providing detailed information on the analytical instruments and chemicals employed in the study. Next, Chapter 4 presents the results of the experimental data, covering the characterization of raw sludge to identify the potential elements, parameter studies for treatment process, and analysis for post-leached residues. Chapter 5, the final section of the report concludes the entire research study and provides potential recommendations for future investigations.

CHAPTER 2

LITERATURE REVIEW

2.1 Introduction

On a global scale, the amount of sludge is projected to increase. This is attributed to growing percentage of industrial activities that being connected to the wastewater treatment plants, more stringent regulation on the effluent discharges, and the advancements in technologies that enhance the efficiency of wastewater treatment process. Despite producing a massive amount of sludge annually, its utilization has not received much attention. Therefore, to make strides in the field of sludge recycling in Malaysia, one crucial aspect that should be taken into account is the characteristics of the industrial sludge. In this context, a fundamental understanding of the properties of the sludge is essential in identifying the most suitable treatment method to extract pollutants from the sludge.

2.2 Sludge Management

The most common pathways of sludge pre-treatment are thickening, dewatering, stabilization and followed by final disposal strategies. It is crucial to eliminate the potential consequences by lowering the pathogenic organisms in the organic matters (Rorat, et al., 2019). Otherwise, it would be extensively unfeasible to deal with the sludge for the succeeding process (Qrenawi and Rabah, 2021).

2.2.1 Moisture Removal

A series of sludge moisture removal which include thickening, dewatering and drying are essential to make it more manageable. Although these processes differ from each other in terms of their mechanism, technology and end product, they share a common objective to reduce the water content in the sludge, while increasing the solid concentration. According to Kamizela and Kowalczyk (2019), the method of water removal primarily relies on the nature of the water content within the sludge, as outlined in Table 2.1 below. Not only that, but Figure 2.1 depicts the types of water bound within the sludge.

Table 2.1: Types of Water in Sludge with its Removal Process Processing (Dichtl and Kopp, 2000; Novak, 2006; Kamizela and Kowalczyk, 2019).

Types of Water	Description	Removal Process
Free Water	water that moves freely between the sludge particles and is not bound to them.	Gravitational Thickening
Interstitial Water	water trapped within the sludge floc by capillary forces.	Mechanical Dewatering
Bound Water (Hydration Water)	intracellular water presents only in the cell.	Partially via mechanical dewatering; Thermal Process
Vicinal Water	water that held on the solid surfaces.	Drying

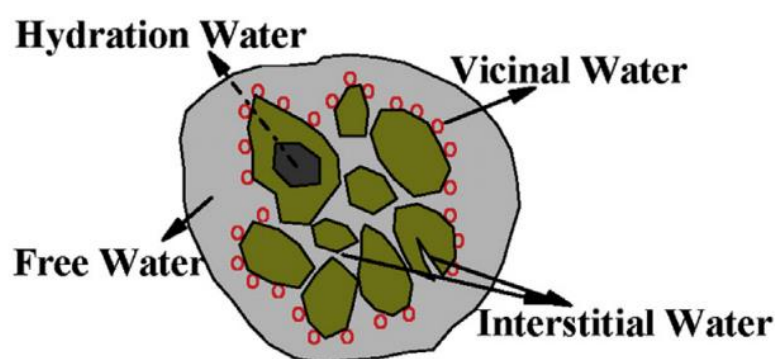


Figure 2.1: Water Distribution Inside the Sludge (Guangyin and Youcai, 2017).

On top of that, the effectiveness of the sludge dewatering process is significantly impacted by its water content or solids concentration after being treated (Ginisty, et al., 2016). Table 2.2 presents a comparison of the thickening, dewatering and drying processes, in terms of the moisture content remained in the treated sludge, as well as the solid content can be recovered for each mechanism.

Table 2.2: Comparative Analysis of Sludge Moisture Removal Processes.

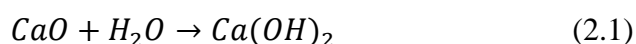
Process	Description	Moisture (%)	Method	Mechanism	Solid Content (%)	Reference
Thickening	To reduce volume for subsequent process. Product still in liquid behaviour.	92-94	Gravitational Settling	Natural settling of particles due to gravity and density differences with liquid.	4-6	(Kamizela and Kowalczyk, 2019)
			Flotation	Solids attach to microscopic air bubbles and float to the surface for removal.	3-4	(Dentel and Qi, 2013)
			Rotary Centrifugation	High speed centrifugal force to separate solids from liquid.	5-7 (without polyelectrolytes) 6-8 (with polyelectrolytes)	(Kamizela and Kowalczyk, 2019)

Table 2.2 (Continued)

Process	Description	Moisture (%)	Method	Mechanism	Solid Content (%)	Reference
Dewatering	Further remove the moisture in sludge to form a solid cake.	60-85	Belt Filter	Pressure to expel water from sludge on the porous belt through compression, while retaining solids.	15-25	(Qrenawi and Rabah, 2021); (Dentel and Qi, 2013)
			Pressure Filtration	High-pressure pumps drive solids into the press, where rising pressure expels liquid through discharge ports.	25-35	(Dentel and Qi, 2013)
			Decanter Centrifuges	Scroll discharge in a solid bowl while decanting the liquid.	12-19	
Drying	To attain an appropriate water content for subsequent sludge processing.	≤ 10	Thermal Drying	<p>Direct Drying: direct thermal contact with heating medium.</p> <hr/> <p>Indirect Drying: agitation or scraping of sludge from a hot surface.</p>	55-95	(Gross, 1993); (Chen, Yue and Mujumdar, 2002); (Aziz and Mustafa, 2022)

2.2.2 Lime Stabilization

Lime stabilization is accomplished chemically by adding quicklime (CaO) into the sludge at a sufficient dose to produce an extremely alkaline pH (Grobela, Czerwińska and Murtaś, 2019). The reaction is shown as Equation 2.1.



The reaction is exothermic in nature, resulting in a temperature elevation of over 30 °C. This rise in temperature plays a pivotal role in deactivating any potential pathogenic organisms that might be present within the sludge. Furthermore, Dentel and Qi (2013) asserted that the alkaline condition leads to the deprotonation of acidic odorants like hydrogen sulfide (H₂S), which eventually diminishes odor intensity. Besides, the condition facilitates the saponification of fats, oils and grease (FOG) to their lower molecular weight derivatives, thereby enhancing their biodegradability.

2.2.3 Aerobic Digestion

Aerobic digestion of sludge involves the aerobic microorganisms to metabolize the biologically degradable organic constituents within the sludge in the presence of oxygen (Bernard and Gray, 2000). Under the aerobic conditions, bacteria efficiently consume the organic matter, converting it into carbon dioxide. The sludge is typically aerated with oxygen at a thermophilic temperature, surpassing 50 °C. This process facilitates the removal of volatile solids, achieving a potential reduction of up to 38 % (Anjum, Al-Makishah and Barakat, 2016). Moreover, Grobela, Czerwińska and Murtaś (2019) shared the similar view, noting that around 40 % of volatile solids are typically diminished through this approach. However, aerobic digestion is commonly employed in smaller treatment facilities, as this method does not result in energy recovery, and tends to be more costly due to the continued aeration.

2.2.4 Anaerobic Digestion

Anaerobic digestion is a complicated biological process which involves several stages of biotransformation of organic matter, including hydrolysis, acidogenesis, acetogenesis and methanogenesis in the absence of oxygen (Aziz

and Mustafa, 2022). A basic diagram showcasing the anaerobic digestion process for sludge stabilization is depicted in Figure 2.2. Most high-rate digesters are operated within the mesophilic temperature range, typically maintained between 30 and 38 °C. However, it can also occur at higher temperatures known as the thermophilic region, ranging between 50 and 57 °C. This range is conducive to the growth of thermophilic bacteria, making it suitable for their metabolic activity and the ensuing digestion processes (Appels, et al., 2008). According to Anjum, Al-Makishah and Barakat (2016), high caloric biogas with over 60 % of methane will be achieved through the transformation of excessive organic compounds present in the sludge. The generated biogas holds potential for diverse applications, including building heating, electricity generation, and potentially serving as vehicle fuel if cleaned to natural gas quality (Dentel and Qi, 2013).

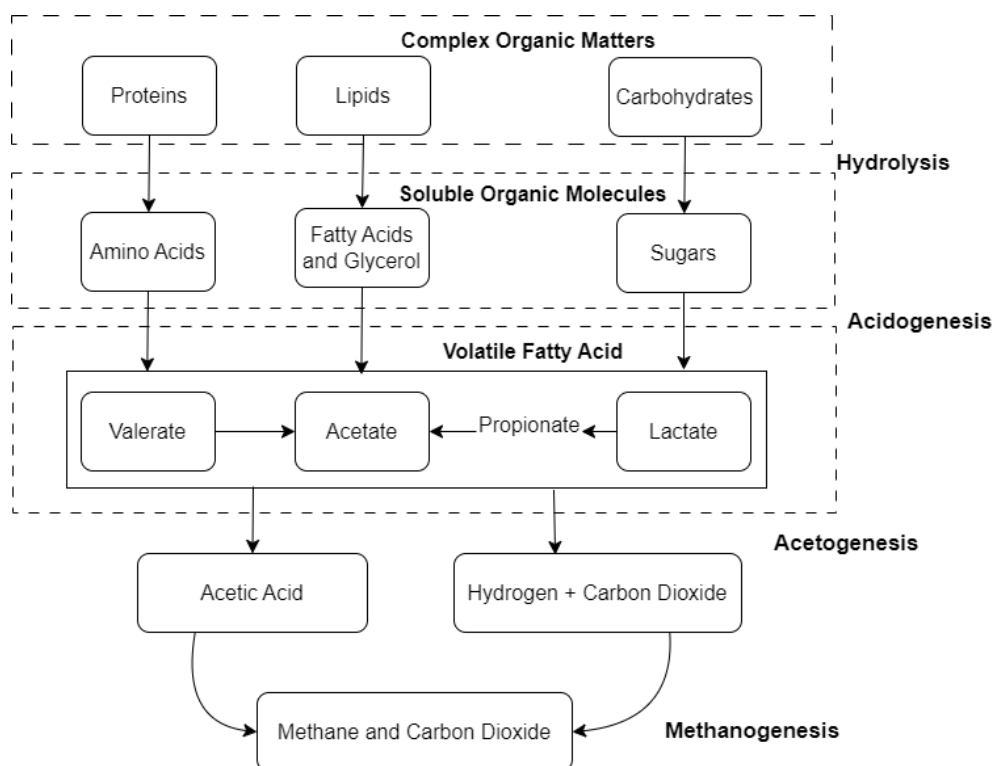


Figure 2.2: Simplified Diagram of Anaerobic Digestion (Dentel and Qi, 2013).

2.3 Characterization Study of Sludge

2.3.1 Fourier-Transform Infrared Spectroscopy (FTIR)

FTIR analysis is a prominent spectroscopic approach used to identify and characterize the functional groups within a sample by measuring the interaction of molecules with infrared radiation. When a specific functional group is irradiated with a specific wavelength of light, its chemical bond absorbs energy and vibrates at certain frequencies either through stretching or bending (Daeid, 2005). The output of the detector will generate an interpretable spectrum displaying the frequency of light and their absorbance, allowing for the identification of functional groups within the sample.

In the recent research by Billah, Techato and Taweepreda (2020), the functional groups presented in the concentrated latex sewage sludge (CLS) were characterized. It mostly consisted of aliphatic side chains, aromatic nuclei and oxygen-containing groups such as hydroxyl and carbonyl groups. Table 2.3 presents the findings.

Table 2.3: Functional Groups in CLS.

Wavelength (cm^{-1})	Transmittance (%)	Functional Group	Class
673.13	1.20	C-H bond bending in the aliphatic side chain	Alkane
757.99	1.23		
875.64	1.22		
908.43	1.22	C=C bending in the aromatic group	Alkene
1037.79	1.13		Amide
1195.81	1.28	C=O bond stretching vibration	Ester
1521.77	1.28		Amide
1623.99	1.28	C=C stretching	Alkene
2108.10	1.37	C \equiv C stretching	Alkyne
2923.95	1.32	C-H stretching in the aliphatic side chain	Alkane
3286.55	1.32	O-H stretching	Alcohol

Besides, the FTIR spectrum of the natural rubber (NR) graded TSR3CV had been studied by Rolere, et al. (2015), as illustrated in Figure 2.3. The result featured five prominent bands associated with non-isoprene compounds, namely amine (3283 cm^{-1}), ester ($1738 - 1748\text{ cm}^{-1}$), carboxyl (1711 cm^{-1}), amide I (1630 cm^{-1}) and amide II (1541 cm^{-1}).

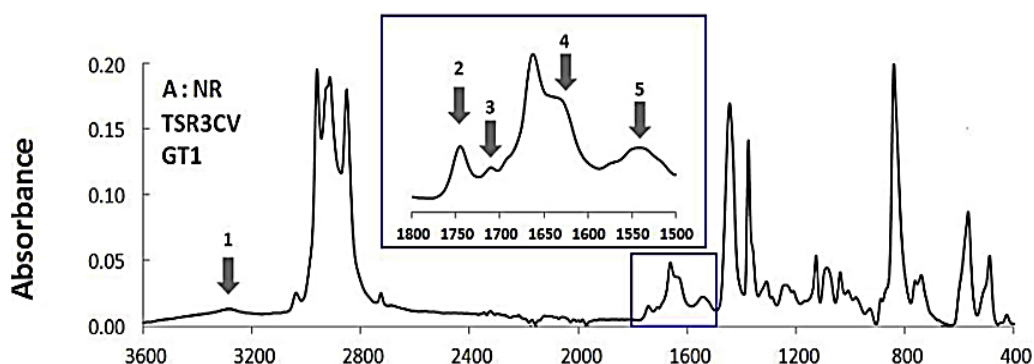


Figure 2.3: FTIR Spectrum of Natural Rubber (Rolere, et al., 2015).

For both CLS and NR, the common vibrational bands contributed to the carbon-carbon and carbon-hydrogen bonds (Rolere, et al., 2015). It could possibly be attributed to the presence of isoprene monomer, which is a main constituent in the rubber compound (Gunasekaran, Natarajan and Kala, 2007). Figure 2.4 demonstrates the chemical structure of the isoprene monomer.

In addition, the non-isoprene compounds such as amine, ester, carboxyl, as well as amide group were present in both samples. These compounds might come from the additives introduced during the rubber manufacturing process. For example, the isoprene monomer was hydroborated to add hydroxyl group prior to esterification process with stearic acid in order to increase the crystallization rate (Kakubo, et al., 1998). In view of the presence of amine group (N-H) in NR, it might be contributed by the addition of stabilizer into the NR. This stabilizer, often in the form of neutral hydroxylamine sulfate, serves the purpose of mitigating storage hardening concerns (Rolere, et al., 2015).

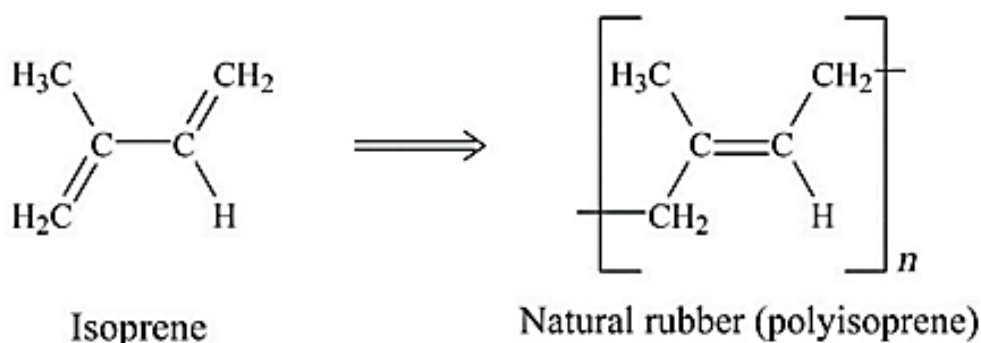


Figure 2.4: Chemical Structure of Isoprene (Ali Fazli and Rodrigue, 2020).

2.3.2 Scanning Electron Microscopy-Energy Dispersive X-Ray (SEM-EDX)

SEM analysis entails utilizing an electron microscope to produce a high-resolution image of the sample's surface. Meanwhile, EDX analysis is performed to determine the elemental composition of the sample. X-rays in a SEM can be generated in two steps. Firstly, the electron beam will strike the inner shell of the sample, thereby transferring some of its energy to the atom of the sample. With the received energy, the electron of the atom leaps to a higher energy shell, leaving a positively charged electron vacant. As a result, it attracts a negatively charged electron from the outer shell to fill the vacancy. An X-ray can be released as an outcome of the energy difference of this transition (AZO Materials, 2018). The EDX detector will then examine the X-ray, allowing it to identify the elemental composition. Since each element emits a unique type of X-ray spectrum, the elements can be differentiated from one another (measurlabs, 2023).

The analysis of rubber waste through SEM-EDX have been proposed by few authors. The SEM images of the rubber waste from different sources are displayed in the Figure 2.5. All the rubber wastes exhibited a non-uniform size and irregular shape. Nevertheless, the recycled rubber waste in Figure 2.5 (a) had rougher surface than the crushed rubber crumb in (b). Additionally, for the highlighted part in (b) and (c), thread-like fiber elements had been found in raw and crushed rubber crumb, due to the inclusion of reinforcing fibers from the used automotive tyres. Apart from that, the elements on the surface of these rubber waste with their weight percentage are summarized in the Table 2.4.

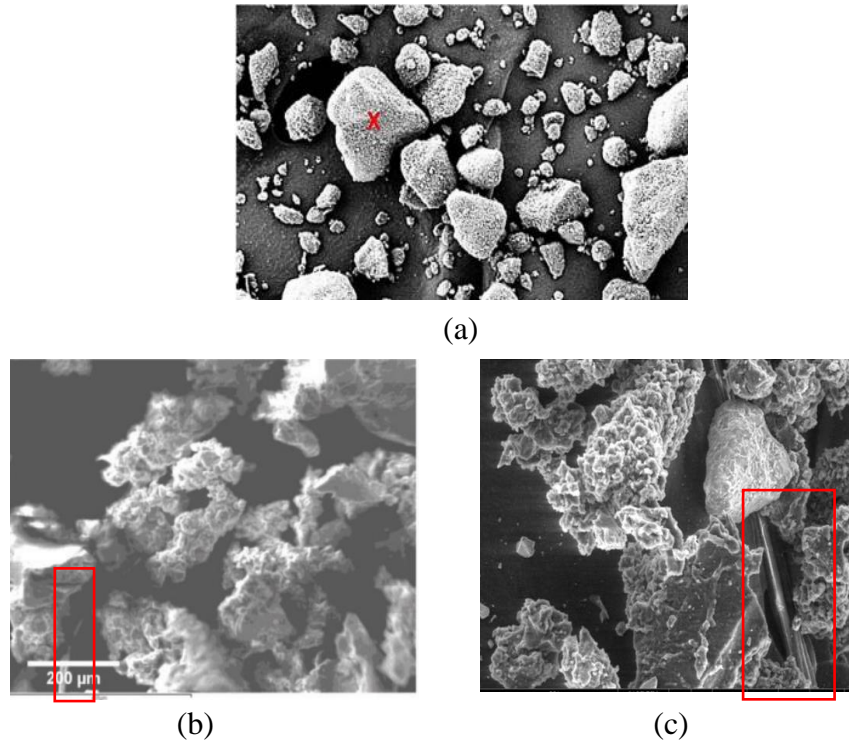


Figure 2.5: SEM Images of (a) Recycled Rubber Waste (Abbas, et al., 2022), (b) Raw Rubber Crumb (Haworth, et al., 2018) and (c) Crushed Rubber Crumb (Bisht and Ramana, 2017).

Table 2.4: Elemental Analysis for Rubber Wastes.

Elements	Percentage (%)		
	Recycled Rubber Waste	Raw Rubber Crumb	Crushed Rubber Crumb
Carbon (C)	74.83	82.7	87.50
Silicon (Si)	9.90	0.89	0.20
Aluminium (Al)	2.15	-	0.08
Zinc (Zn)	0.82	6.34	1.77
Magnesium (Mg)	0.26	-	0.14
Sulfur (S)	0.87	2.07	1.07
Oxygen (O)	11.17	8.02	9.24

The rubber waste mainly constituted of carbon (C), as it is a crucial element in the composition of rubber macromolecules. The detected Al may be due to the application of metallic cords to reinforce the rubber product. Apart

from that, sulfur plays the role of vulcanization agent for the crosslinking of rubber compounds, while zinc oxide (ZnO) acts as the vulcanization activator (Haworth, et al., 2018). Furthermore, silica is always dosed to a polymer in order to enhance its mechanical and physical properties (Aoudia, et al., 2017).

2.3.3 X-ray Diffraction (XRD)

The core components of X-ray diffractometers include an X-ray detector, an X-ray tube, and a sample holder. First, X-rays with a specific wavelength are produced in a cathode ray tube when it is energized. After that, the sample is targeted by collimating these X-rays. The crystal atoms of the sample will scatter the incident X-rays, primary through the interaction with the electrons surrounding these atoms. The detector will then record the intensity of the diffracted X-rays that pass through various angles (Gotame, 2021).

An XRD analysis studied on the sludge collected from a natural rubber processing industry by Uttara Mahapatra, Ajay Kumar Manna and Abhijit Chatterjee (2022) concluded that the sludge exhibited an amorphous structure with discrete locations of crystalline species. As shown in Figure 2.6, a significant sharp peak was observed at the 2θ values of approximately 26° , indicating that the calcium carbonate (CaCO_3), also known as calcite, possessed the highest intensity in the sludge. Besides, prevalent but low intensity diffraction peaks appeared at around 51° , 55° , 67.8° , 71° , as well as 80° to 85° , which were analogous with characteristic peaks for quartz. The presence of other minerals, such as hematite (Fe_2O_3) at 39° and 61° , as well as dolomite ($\text{CaMg}(\text{CO}_3)_2$) at around 31° and 33.6° , were also detected, albeit in very small intensities. The authors asserted that these crystalline compounds may be derived from the raw materials used during the physicochemical treatment of the rubber.

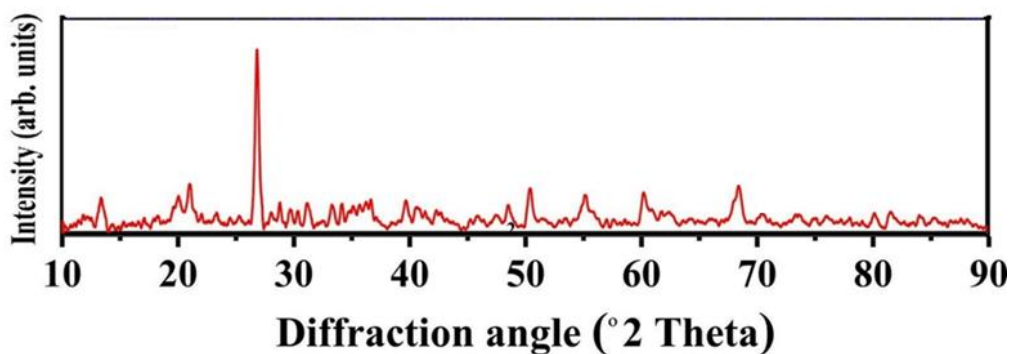


Figure 2.6: XRD Pattern of Rubber Sludge (Uttara Mahapatra, Ajay Kumar Manna and Abhijit Chatterjee, 2022).

The XRD diffractogram of raw crumb rubber, obtained by the analysis carried out by Roychand, et al. (2021) is presented in Figure 2.7. The sample prominently consisted of amorphous organic compound or carbon black, as a broad hump was observed rather than a sharp peak at the angle around 20°. Additionally, the detection of ZnO in a small fraction aligned with the findings of the previously mentioned EDX analysis on rubber sludge. Similar to the rubber sludge mentioned above, CaCO_3 was detected at an angle around 29.4°.

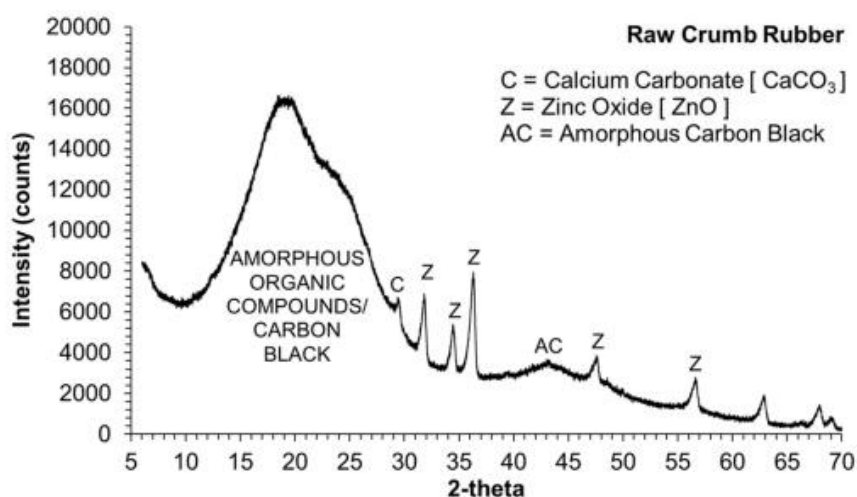


Figure 2.7: XRD Pattern of Raw Rubber Crumb (Roychand, et al., 2021).

2.3.4 Thermogravimetric Analysis (TGA)

TGA is normally carried out to determine the weight change of a sample with respect to temperature and time. Inside a furnace, the temperature of the

sample is steadily raised. Meanwhile, the changes in weight of the sample during the heating process are continuously monitored to link them to various thermal degradation phases (Ng, et al., 2018).

Uttara Mahapatra, et al. (2021) conducted the experiment of TGA using the biosludge (BS) from the rubber industry under nitrogen and air atmosphere. As depicted in Figure 2.8, the TGA profile was divided into three phases.

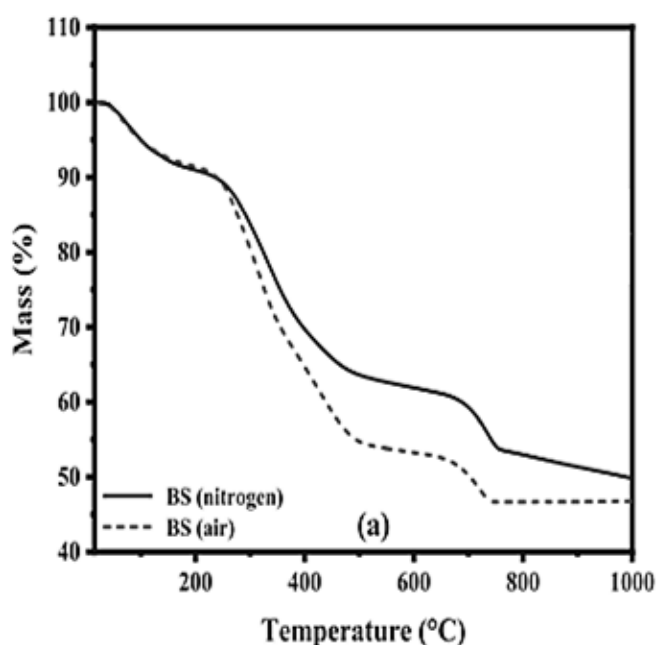


Figure 2.8: TGA under Nitrogen or Air (Uttara Mahapatra, et al., 2021).

The first stage, occurring in the range from 22 to 200 °C, clearly showed overlapping curves under both gases, with up to 8.81 % weight loss. The authors stated that mass loss in this phase was resulted from the evaporation of interstitial water content and absorbed moisture in the sludge.

The second stage covered the temperature range from 200 to 490 °C with 36.25 and 27.05 % weight loss under an environment of air and nitrogen atmosphere, respectively. The weight loss in this phase was mainly contributed to the decomposition of carbonaceous matrix in the sludge. Furthermore, the higher percentage of mass loss observed under the air atmosphere indicated that the decomposition reaction was accelerated by the presence of oxygen.

Apart from that, Silva, et al., (2020) emphasized that the mass loss of natural rubber occurred at 374 °C.

Lastly, the final weight loss occurred in the temperature range from 490 to 1000 °C, primary due to the decomposition of CaCO₃. This result confirmed the findings of the earlier XRD study, which indicated the presence of CaCO₃ at major concentration. In the end, around 46.76 % of residue was found under air condition, whereas 49.84 % under a nitrogen atmosphere.

2.4 Sludge Digestion Study

The most common techniques utilized to quantify the concentration of heavy metals in the samples rely on highly sensitive spectroscopic instruments, including Flame Atomic Absorption Spectroscopy (FAAS), Inductively Coupled Plasma – Optical Emission Spectrometry (ICP-OES), Inductively Coupled Plasma – Mass Spectrometry (ICP-MS). However, a limitation of these methods is their requirement for converting solid samples into aqueous form prior to analysis (Uddin, et al., 2016). To ascertain the total metal content within the sludge, a procedure called acid or wet digestion is necessary to release the metals from solid sludge into acid solution (Egüven and Akinci, 2011). In this context, acid digestion is preferred due to its effectiveness in recovering various analyte contents in highly complex matrices. It has been asserted that environmental samples generally contain silicate, metal oxides, carbonates, as well as organic matter. Therefore, a rational selection of acid or acid mixture is important in order to facilitate the solubilization of these chemical forms (Ramanathan and Ting, 2015).

2.4.1 Single Acid Digestion

In digestion with single acid, the commonly used acids involve concentrated nitric acid (HNO₃), hydrochloric acid (HCl), hydrofluoric acid (HF), and sulfuric acid (H₂SO₄) (Elisabeth, Terry and Azad, 2017). To illustrate, HCl is effective for the compounds in the form of carbonates, phosphates, certain oxides and some sulfides (Egüven and Akinci, 2011). Nevertheless, some elements might form metal precipitates when treated with this acid.

Additionally, HNO₃ serves as a universal reagent, being non-interfering with most determinations as it avoids ionic precipitation

(Matusiewicz, 2003). Besides, it acts as strong oxidizing agent on many organic substances and metal salts, releasing their trace elements as high soluble nitrate salts (Hu and Qi, 2013). Due to its oxidizing capacity, accessibility and affordability for sufficient purity, it is frequently utilized for digestion purposes as an oxidant reagent (Uddin, et al., 2016).

Regarding the use of H_2SO_4 , its primary role is to dehydrate and dehydrogenate the organic material, while providing a high temperature medium for the digestion process (Partridge and Bosuego, 1980). Unfortunately, the low solubility of certain organic sulfates and the volatilization of trace elements during the process limit its widespread use for sample digestion.

In addition, HF is particularly useful for dissolving silicate samples by forming volatile silicon tetrafluoride. Despite its potency in breaking strong silica oxide bonds, HF is seldom employed as the sole reagent due to the poor solubility of most salts (Hu and Qi, 2013). Moreover, HF is among the most hazardous acids, known for its highly corrosive and toxic properties. Its use can result in the gradual deterioration of equipment and instruments over time (Jing, 2004; Watkins, et al., 2018).

2.4.2 Acid Mixtures Digestion

Twyman (2005) claimed that acids mixture is generally more advantageous in decomposing both organic and inorganic matrices. Different combinations of acids can be employed for this purpose. For instance, employing HF alongside another mineral acid with higher boiling point, such as HNO_3 or perchloric acid, proves effective in achieving complete sample decomposition, particularly in the presence of silicates. The inclusion of a second acid with a higher boiling point assists in dissolving sparingly soluble metal fluorides into more soluble salts after the evaporation of HF.

On the other hand, strong attacks but leaving with a residue of certain minerals can be conducted with various mixtures of concentrated HNO_3 , HCl, and H_2SO_4 . To elucidate, a 1:4 mixture of H_2SO_4 and HNO_3 is utilized to digest organic samples. The high boiling point of H_2SO_4 enables it to decompose the organic matter that remains after the nitric acid is boiled off (Twyman, 2005). On top of that, one of the most widely utilized mixtures is

Aqua Regia, a fresh combination of concentrated HNO_3 and HCl in a volume ratio of 1:3. According to Elisabeth, Terry and Azad (2017), despite HCl being a non-oxidizing acid on its own, when mixed with HNO_3 in specific proportions, it transforms into a potent oxidizing agent. The efficacy of this reagent is likely attributed to the catalytic effect of the products resulting from their reaction, namely nitrosyl chloride and chlorine (Hu and Qi, 2013). Aqua Regia is recognized as effective in dissolving a wide range of base element sulfates, sulfides, oxides and carbonates (Gaudino, et al., 2007). Not only that, but for samples containing principally inorganic matrices (Matusiewicz, 2003).

Most authors proposed the modification of acids through the inclusion of strong hydrogen peroxide. Twyman (2005) and Elisabeth, Terry and Azad (2017) claimed that the introduction of hydrogen peroxide can enhance the solubilizing capacity of acids and facilitate the decomposition of organic matter without the risk of explosion. Additionally, Ramanathan and Ting (2015) stated that hydrogen peroxide will accelerate the digestion process through oxidation.

2.5 Metal Removal from Sludge

Sludge obtained from the rubber industry has been categorized as hazardous scheduled waste owing to its high content of heavy metals. According to the research carried out by Rani, et al. (2020), the analysis of raw rubber sludge revealed significant percentages of heavy metals, with aluminium (Al) - 30.3%, zinc (Zn) - 11.7 %, iron (Fe) - 7.1 %, chromium (Cr) - 0.3 % and nickel (Ni) 0.1 %. Table 2.5 highlights several strengths and weaknesses of current technologies used to remove heavy metal from sludge.

Table 2.5: Advantages and Disadvantages of Technologies in Heavy Metals Removal from Sludge (Geng, et al., 2020; Soliman and Moustafa, 2020).

Technologies	Advantages	Disadvantages
Electrokinetic Process	- <i>In situ</i> process	- Long treatment time
	- No introduction of other harmful ingredients	- Poor solubility of metal ions in sludge - High energy consumption - Corrosion of electrodes
Ion-exchange Extraction	- Resin can be regenerated and recycled	- Matrix fouled easily due to concentrated metal
	- High selectivity	- Highly sensitive to pH - Regeneration of resin causes secondary pollution
Biobleaching	- Environmentally friendly	- Microbes are sensitive to temperature and pH - Long leaching time - Infeasible in industrial application
Acid Leaching Treatment	- Speedy - Simplicity - High heavy metal removal efficiency	- Large amounts of chemical agents needed

From the comparison above, it is obvious that acid leaching method emerged as the most promising way due to its simplicity in operation and the requirement for less specialized expertise.

2.5.1 Acid Leaching

Acid leaching had been proposed by several authors. According to Veeken and Hamelers (1999), metal extraction from sludge generally takes place in three stages. The actual extraction process begins with the introduction of acid into

the sludge, which eventually dissociates the metal compounds present, resulting in the existence of metal ions in aqueous form. The process is facilitated by the exchange of protons from the acid, leading to the solubilization of metals in the sludge, as depicted in Equation 2.2 (Lo and Chen, 1990).



In order to separate the aqueous phase from the purified sludge, a solid-liquid separation process is used in the second stage. Subsequently, a series of precipitation and separation processes are performed to separate the metals from the extraction solution. This process is essential to prevent harmful effects on the environment resulting from the discharge of the extracting fluid (Stylianou, et al., 2007).

2.5.2 Effect of Acid on Leaching Rate

Among the organic and inorganic acid, inorganic eluting agents are commonly utilized in the leaching process due to their potent dissolution capabilities. Furthermore, certain inorganic acids possess complexing abilities, allowing them to efficiently remove metals from sludge (Xiao, et al., 2022). A study was carried out by Wu, Kuo and Lo (2004) to assess the efficiency of sulfuric acid, nitric acid and hydrochloric acid in removing the copper, lead, zinc and nickel from industrial sludge. Under 1 N extractants, the results proved that the extraction efficiency followed the order: sulfuric acid > nitric acid > hydrochloric acid. On top of that, Widi Astuti, et al. (2016) also stated that sulfuric acid emerged as a more favourable reagent due to its ability to produce twice as many hydrogen ions (H⁺) as nitric acid and hydrochloric acid under equivalent concentration.

2.5.3 Effect of Time on Leaching Rate

Wahab, et al. (2021) observed a positive relationship between leaching duration and the percentage of metal extraction, with longer durations leading to higher extraction rates. This finding was further supported by Alkan, et al. (2018), who stated that the leaching process is primarily controlled by

diffusion. Therefore, an extended contact time between the acid and the sample is believed to contribute to a more substantial yield of the extracted product.

Cao, et al. (2018) conducted an investigation to assess the leaching efficiency of three rare earth elements in fly ash under constant conditions, spanning a duration range of 30 to 180 minutes. The results revealed that the leaching efficiency was categorized into four distinct stages, which have been summarized in Table 2.6.

Table 2.6: Leaching Efficiency over Time.

Stage	Duration (min)	Efficiency (%)	Reason
1	≤ 60	exponentially	The combination of a high concentration of H^+ in the reagent solution and a high content of compounds in the sample resulted in a rapid leaching process.
2	60 – 90	almost unchanged	Surface compounds were completely leached, while unreacted part was mainly tightly packed within samples. Leaching was only possible after H^+ diffusion.
3	90 – 120	increased dramatically	The diffusion process occurred within the sample particles, wherein H^+ came into contact with easily dissociable compounds contained within.
4	≥ 120	slow	The remaining concentration of H^+ decreased, hindering the dissociation of unreacted compounds.

2.5.4 Effect of Temperature on Leaching Rate

The ideal leaching temperature have to be considered to maximize the extraction yield, meanwhile, reducing the energy consumption. There is a proportional relationship between temperature and metal extraction efficiency.

To explain it, firstly, dissolution reaction is generally endothermic, thereby higher temperature enhances this reaction (Chi, et al., 2006). In addition, higher temperature will cause the average kinetic energy between the molecules to rise, leading to more frequent and energetic collisions, and further enhancing the leaching reaction. Arrhenius equation with Equation 2.3 can be applied to explain this relationship between the rate constant and temperature (Wahab, et al., 2021).

$$\ln k = \ln A - \frac{E_a}{RT} \quad (2.3)$$

where

k = rate constant

T = temperature, K

A = frequency factor

E_a = activation energy, J/mol

R = gas constant, $8.314 J/mol \cdot K$

Mirwan, et al. (2020) conducted an assessment of the Al extraction rate from clay across temperatures of 30, 50, 70, and 90 °C. The study revealed a notable increase in Al recovery percentage, reaching up to 91 % at 90 °C, in contrast to a significantly lower recovery of only 16 % at 30 °C. The outcomes are graphically represented in Figure 2.9, showcasing a similar pattern to a study by the same authors, Mirwan, et al. (2017), who explored the leaching of Al from water treatment sludge. This eventually highlighted the significant influence of temperature on the extraction efficiency for metals from the sample.

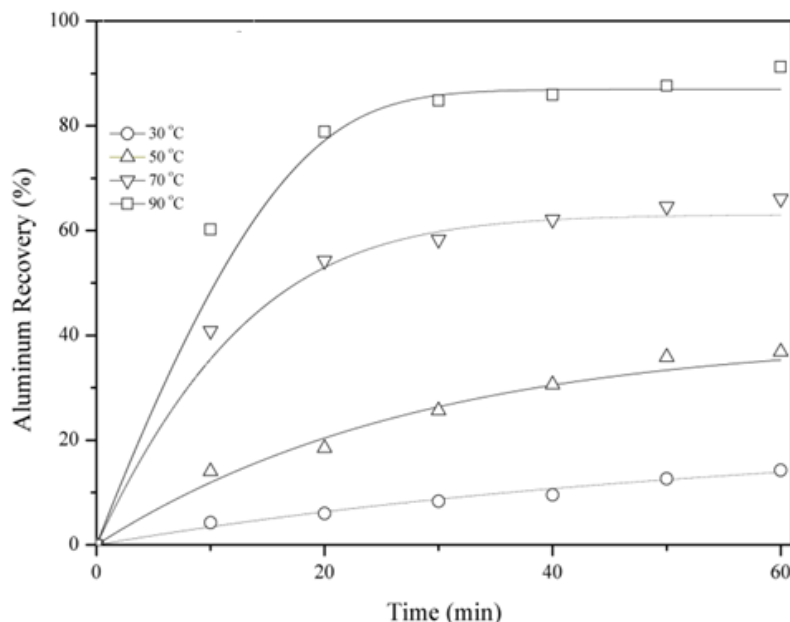


Figure 2.9: Leaching Efficiency of Al Under Different Temperature.

2.5.5 Effect of Acid Concentration on Leaching Rate

An optimum acid concentration should ensure that the reagent diffusion rate equivalent to the reaction rate (Chi, et al., 2006). According to Hosseini, et al., (2017), the activity of hydrogen ions, H^+ increases with acid concentration, leading to more dissolution of metal into aqueous solution. In accordance with the Le Chatelier's Principle, the reactivity of materials containing metal with acid will shift to the right with increasing acid concentration, thereby increasing the leaching amount.

In this context, Stylianou, et al., (2007) conducted an analysis on the extraction percentages of nickel (Ni), copper (Cu), chromium (Cr) and lead (Pb), considering different concentration of acid in relation to contact time. The results are illustrated in Figure 2.10, indicating that the efficiency of metals recovery was notably higher when using a 20 % v/v H_2SO_4 solution compared to using only a 10 % v/v acid concentration. As an illustration, at a temperature of 80 °C, Cu demonstrated a significantly higher total recovery percentage of 86 % when subjected to a 20 % v/v H_2SO_4 concentration. In contrast, at a 10 % v/v concentration, the total recovery percentage dropped to 55%.

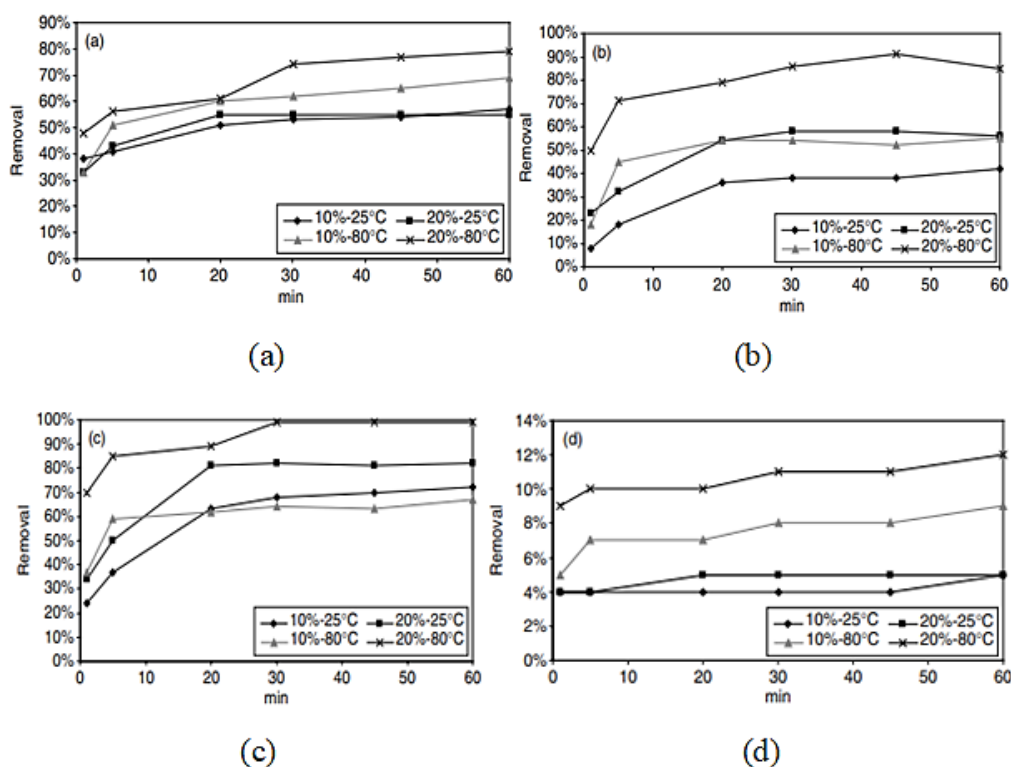


Figure 2.10: Leaching Efficiency of (a) Ni, (b) Cu, (c) Cr and (d) Pb.

2.5.6 Effect of Liquid-to-Solid Ratio on Leaching Rate

The liquid-to-solid ratio (L/S) is a crucial technical parameter in the leaching process, denoting the specific proportion of acid solution to the sludge particles. A higher L/S ratio indicates a larger amount of liquid in the mixture, which reduces viscosity and enhances mass transfer during leaching process. This facilitates the quick diffusion of metal ions from the solid phase to the liquid phase, promoting more effective metal extraction from the sludge (Su, Liang and Guan, 2016). However, if the ratio is excessively low, it reduces the effective surface area for the sample to participate in the reaction, ultimately reducing the leaching rate (Yang, et al., 2023)

The research conducted by Widi Astuti, et al. (2016) demonstrated a remarkable improvement in the leaching efficiency of manganese with a high L/S ratio. The efficiency increased from 66.32 % to an impressive 97.02 % when the L/S ratio was raised from 2:1 to 5:1. Similarly, Su, Liang and Guan (2016) observed a rising trend in the leaching rate of Al, Cu, and Fe from the sludge as the L/S ratio gradually increased from 3:1 to 10:1. Furthermore, the study by Kuan, Lee and Chern (2010) showed that the final heavy metal

residues increased with a higher solid-to-liquid ratio, which brought the meaning that most of the metals remained unrecovered in the sample. This substantial enhancement highlights the significance of selecting a higher L/S ratio to achieve a more effective leaching rate.

2.5.7 Optimum Combination of the Factors

The leaching efficiency is influenced by a combination of several key parameters, as mentioned above (Stylianou, et al., 2007). As a result, direct comparisons between results from various studies become challenging due to the complex interplay of these factors. In this regard, Table 2.7 provides a summary of the percentage removal of the most common metals found in the sludge using different acids, as investigated under various combinations of factors, from different studies.

Table 2.7: Comparison of Metals Removal Efficiency.

Operating Condition	Sludge	Metals Removal Efficiency (%)							Reference
		Fe	Ni	Cu	Cr	Cd	Zn	Pb	
0.5 M H ₂ SO ₄ ; 120 min; 103 °C; 5:1 L/S	Printed-Circuit Board Manufacturing Wastewater Treatment Plant (WTP)			> 99.9				-	(Kuan, Lee and Chern, 2010)
20 % v/v H ₂ SO ₄ ; 30 min; 80 °C; 5:1 L/S	Municipal WTP	-	74.0	86.0	99.0	-	72.0	11.0	(Stylianou, et al., 2007)
20 % v/v H ₂ SO ₄ ; 60 min; 25 °C; 5:1 L/S		-	80.0	50.0	97.5	-	70.0	50.0	
20 % v/v HNO ₃ ; 60 min; 25 °C; 5:1 L/S	Sewage Treatment Plant	-	81.0	22.0	78.0	-	55.0	55.0	(Naoum, et al., 2001)
20 % v/v HCl; 60 min; 25 °C; 5:1 L/S		-	87.0	45.0	98.0	-	68.0	60.0	
1 N H ₂ SO ₄ ; 60 min; 25 °C; 100 g/30 ml S/L		55.0	72.0	20.0	29.0	57.0	78.0	37.0	
1 N HNO ₃ ; 60 min; 25 °C; 100 g/30 ml S/L	Biopolymer Sewage Treatment Plant	42.0	75.0	24.0	27.0	52.0	74.0	100.0	(Yoshizaki and Tomida, 2000)
1 N HCl; 60 min; 25 °C; 100 g/30 ml S/L		54.0	77.0	56.0	28.0	60.0	86.0	100.0	

Table 2.7 (Continued)

Operating Condition	Sludge	Metal Removal Efficiency (%)							Reference
		Fe	Ni	Cu	Cr	Cd	Zn	Pb	
H ₂ SO ₄ ; 20 hrs; 25 °C; 400:1 L/S	Sewage Treatment Plant	-	75.0	57.8	20.3	-	82.3	27.6	(Mingot, et al., 1995)
HNO ₃ ; 20 hrs; 25 °C; 400:1 L/S		-	73.6	65.5	18.9	-	72.1	45.1	
HCl; 20 hrs; 25 °C; 400:1 L/S		-	63.6	60.7	13.2	-	85.9	30.7	
1 N H ₂ SO ₄ ; 4 hrs; 25 °C; 2:1 L/S	Industrial WTP	-	98.9	9.5	97.3	96.9	50.1	36.0	(Lo and Chen, 1990)

2.6 Hydrocarbon Recovery

Oil is found in rubber sludge due to a variety of processes used in the production and processing steps of rubber. For instance, during molding operations to transfer an elastomer into a usable product, lubricants and oils are typically applied to the rubber as mold release agents. In addition, some rubber formulations require the use of plasticizers to increase the raw polymer's flexibility and make it easy to mold, which may directly introduce oil-based components into the rubber. As a result, oil may end up as part of the sludge.

2.6.1 Solvent Extraction Method

Significant advancements have been made in oil recovery technologies for treating oily sludge. Several innovative approaches have emerged, including the freeze-thaw method, solvent-extraction method, pyrolysis, mechanical centrifugation, froth flotation, and electrokinetic techniques. Among these, solvent extraction stands out as the most promising and viable approach for effective oil recovery (Thong, et al., 2021). It is because solvent extraction is one of the most affordable, fastest and most effective techniques for recovering oil (Hui, et al., 2020).

Solvent extraction ensures complete and precise blending of oil within sludge with the extraction solvent to remove non-volatile or semi-volatile organic compounds. This approach relies on the varying solubility of distinct components in the sludge when exposed to different extractants. After mixing the sludge and solvent, the mixture undergoes filtration to eliminate any solids. Subsequently, the filtrate is subjected to distillation, resulting in the recovery of the oil product from the bottom of the distillation apparatus (Zubaidy and Abouelnasr, 2010).

2.6.2 Effect of Solvent on Removal Efficiency

Selecting an appropriate solvent is crucial to achieve high solubility and extraction efficiency of hydrocarbon component within the sludge. Between the non-polar solvent and polar solvent, Nezhdbahadori, et al. (2018) suggested that the non-polar solvents tend to have higher oil recovery rate. This is because the hydrocarbon molecules in the sludge are predominantly

non-polar. To elucidate, non-polar solvents form stronger binary interactions with these non-polar molecules, facilitating a more efficient extraction process. Besides, Latif Ahmad, et al. (2002) studied the performance of six types of organic solvents, namely hexane, benzene, ether, pentane and heptane, while exploring the key parameters influencing the extraction process. Their findings revealed that hexane exhibited the best extraction efficiency, recovering about 0.54 g of oil, compared to only 0.28 g with heptane. Moreover, Thong, et al. (2021) highlighted hexane offered the best recovery efficiency at approximately 68 %, attributing it to being the most-used solvent for oil extraction due to its lower boiling point and higher solubility. Notably, these results contrasted with the outcome of Abouelnasr and Zubaidy (2008), suggesting higher oil recovery percentages with heptane due to its higher molecular weight. This difference may be attributed to the varying composition of oil present in the sludge being investigated.

2.6.3 Effect of Duration on Removal Efficiency

The extraction duration is pivotal in determining extraction efficiency for two fundamental reasons. Firstly, it is crucial to allocate adequate time for the solvent to effectively dissolve the oil present in the processed sludge. Secondly, the duration must also allow ample time for other contaminants or impurities to aggregate into larger particles, facilitating their subsequent separation during the filtration process (Rincón, Cañizares and García, 2005). According to their findings, with the used of different organic solvents, including 2-pentanol, 2-propanol and methyl ethyl ketone (MEK), the extraction yield increased with time and eventually reached a plateau after 20 minutes, indicating that the system had achieved equilibrium. Nevertheless, when using the 2-pentanol as the solvent, there was a gradual decrease in efficiency over time until approximately 25 minutes and remained constant. This behaviour could be attributed to the higher viscosity of 2-pentanol, which impeded the dissolution process of the oil.

2.6.4 Effect of Solvent-to-Sludge ratio on Removal Efficiency

The oil extraction efficiency typically increases with the solvent-to-sludge (S/S) ratio until reaching an equilibrium point. This phenomenon is attributed

to the fact that elevating the S/S ratio enhances the mutual solubility of oil in the solvent, thereby resulting in a higher amount of oil being recovered (Thong, et al., 2021). To further illustrate it, Hu, Li and Hou (2015) conducted an experiment employing four different solvents, namely cyclohexane, dichloromethane, MEK, and ethyl acetate, to investigate the impact of the S/S ratio. The findings exhibited a gradual increase in the oil recovery rate when ratio rose from 1:1 to 8:1. To explain, when using cyclohexane as the solvent, the rate of recovery increased from 26 ± 1.5 to 40 ± 0.5 % as the S/S ratio was raised to 4:1. However, beyond this point, the recovery rate reached a plateau, showing minimal or negligible improvement. Furthermore, Zubaidy and Abouelnasr (2010) conducted a study utilizing Liquified Petroleum Gas (LPG) condensate as the solvent and investigated different S/S ratios ranging from 1:1 to 6:1. Their findings indicated that the optimum S/S ratio for oil recovery was also 4:1, as the percentage of recovery increased from 12.6 to 32.4 %. Beyond this ratio, the percentage recovery of oil exhibited a decline to 30.5 %. This alignment between different studies reinforced the significance of the 4:1 S/S ratio in achieving the highest oil recovery efficiency.

2.6.5 Optimum Combination of the Factors

It is always necessary to delve into the interaction between the S/S ratio, contact time and the types of solvents to identify the most efficient combination for oil recovery from sludge. It is mainly due to the reason that depending solely on only one parameter may overlook the potential synergistic effects, thereby hindering the development of an optimized extraction strategy. Table 2.8 presents a compilation of studies from various literatures, revealing the optimal conditions that yielded the highest recovery efficiency using different types of solvents.

Table 2.8: Comparison of Oil Recovery Efficiency using Solvent Extraction.

Solvent	Duration (min)	S/S Ratio	Efficiency (%)	Source
Hexane	30	0.33 (Sludge to Solvent Ratio)	67.8	(Taiwo and Otolorin, 2009)
Kerosene			63.3	
MEK	120	6:10	39.0	(Dana Abouelnasr and Isam Zubaidi, 2008)
LPG Condensate			32.0	
Heptane			28.0	
Hexane			22.0	
Propanol			12.0	
Iso-butanol			8.0	
Dichloromethane (DCM)			30	
Cyclohexane	30	4:1	41.5	(Hu, Li and Hou, 2015)
MEK			35.0	
Ethyl Acetate			36.6	
2-Propanol			18.0	
DCM			36.8	
2-Propanol	20	2 g/g	78 ±1.5	(Rincón, Cañizares and García, 2005)
2-Butanol			93 ±1.5	
MEK			92 ±1.5	

CHAPTER 3

METHODOLOGY AND WORK PLAN

3.1 List of Materials and Equipment

Prior to carry out the experiment, a comprehensive preparation phase for the chemicals and materials involved is undertaken. Not only that, preparation, characterization and treatment of sludge necessitated the utilization of specialized apparatus and equipment. In the subsections of 3.1.1 and 3.1.2, these components have been presented.

3.1.1 Materials and Chemicals

The sludge generated from the wastewater treatment plant in a local rubber industry was used as the sample to be characterized and purified in this experiment. Table 3.1 lists the chemicals with their purity and respective brand that applied in this research.

Table 3.1: Chemicals Used in the Experiment.

Chemicals	Brand	Purity	Usage
Sulfuric Acid (H ₂ SO ₄)	Chemiz	95 %	- Leaching Process
Hydrochloric Acid (HCl)	Merck	37 %	- Digestion of Sludge - Leaching Process
Nitric Acid (HNO ₃)	Chemiz	69 %	- Digestion of Sludge - Leaching Process

3.1.2 Equipment and Apparatus

To conduct this experiment, various equipment and apparatus were utilized, as listed in Table 3.2.

Table 3.2: Apparatus and Equipment Used in the Experiment.

Apparatus/ Equipment	Specification	Purpose
Oven	Memmert	Drying of sludge.
Sieve	300 μm -mesh size	Sieving to get a consistent size range.
Heating Mantle	Mtops	Maintain the desired temperature during the leaching and digestion process.
Scanning Electron Microscope Equipped with Energy Dispersive X-ray (SEM-EDX)	Hitachi S-3400N	Determination of surface morphology and elemental composition in the sludge.
X-ray Diffractometer (XRD)	Shimadzu XRD-6000	Analysis for the crystalline structure of the sludge.
Fourier Transform Infrared Spectrometer (FTIR)	Nicolet IS10	Identification of the functional groups present in the sample.
Thermogravimetric Analyzer (TGA)	Perkin Elmer STA8000	Determination of thermal stability of the sludge.
Inductively Coupled Plasma Optical Emission Spectrometry (ICP-OES)	Perkin Elmer Optima 7000	Determination of metals content in the leachate solution.

3.2 Overall Flowchart

Figure 3.1 provides a comprehensive depiction of the overall process in this study. Some steps were repeated, if necessary, to achieve the optimum conditions in leaching of most abundant inorganic elements from the sludge sample.

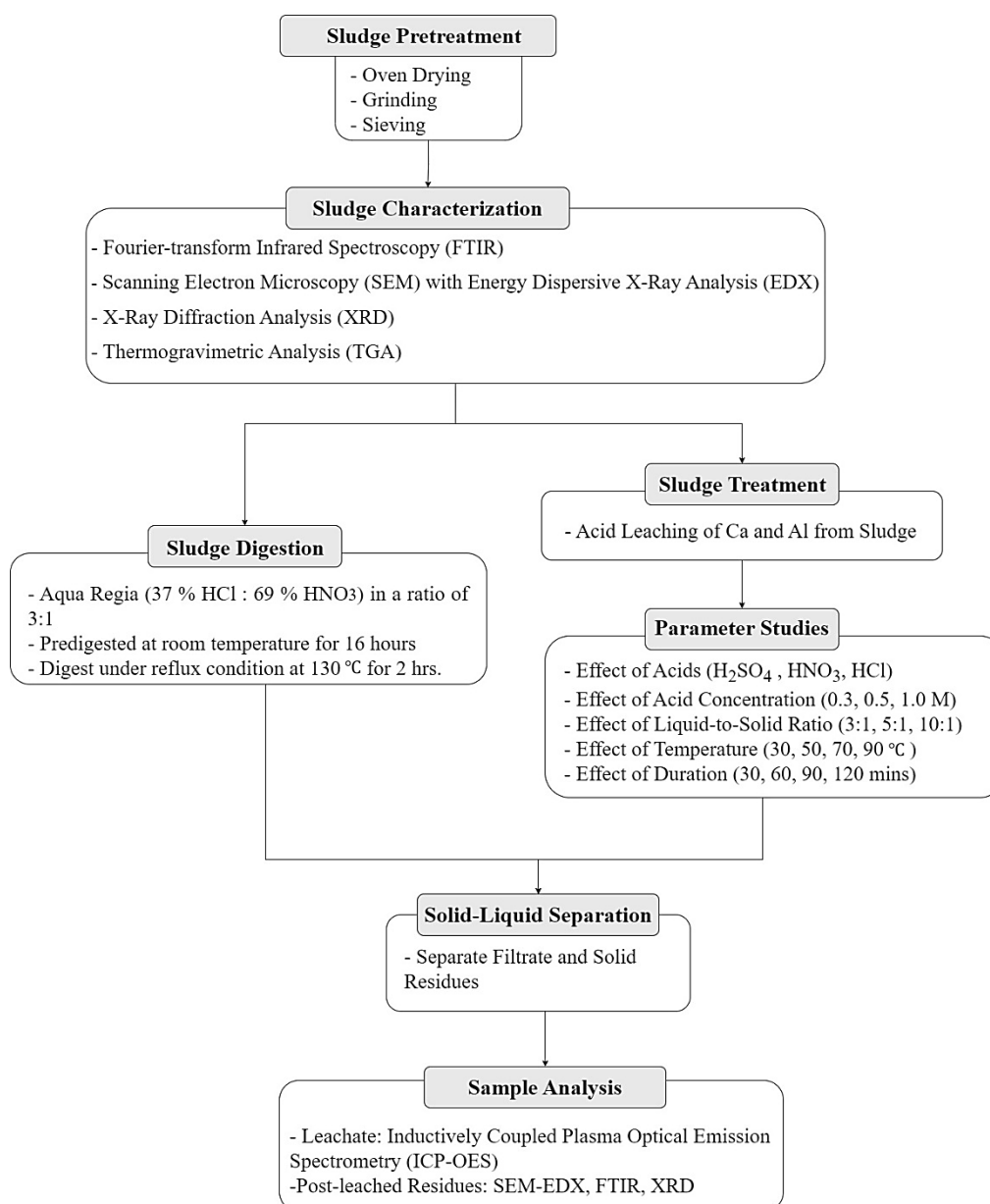


Figure 3.1: Flow Chart of Overall Study.

3.3 Pre-Treatment of Sludge

The sludge was dried at 105 °C for 24 hours by using a Memmert model oven. Next, the dried sludge was grinded into powders using powder grinding machine to reduce the sample size and increase the specific surface area. The powders were then screened through a 300 µm-mesh sieve to achieve a more homogenous mixture. The resulting sample was collected and kept in a well-sealed container before using for the following characterization analysis.

3.4 Characterization Study of Sludge

Characterization of sludge was carried out using various analytical instrument to gain a comprehensive understanding of its chemical and physical properties. In this context, different analytical techniques provide unique insight into different aspects of sludge, enabling informed decision-making regarding the treatment process.

3.4.1 FTIR

FTIR spectroscopy is a powerful instrument to analyze the vibrational energy levels of sample molecules. FTIR Spectrometer model Nicolet IS10 supplied from ThermoFisher Scientific was used to analyze the rubber sludge. The sample powder was pressed into pellet and held at the fixed position in the sample holder by using the pressure tower and compression tip. The FTIR spectra were then captured at a resolution of 4 cm^{-1} and 254 scans in the spectral region of $4000 - 400\text{ cm}^{-1}$. The functional groups and their percentage transmittance were then identified.

3.4.2 SEM-EDX

Elemental composition and surface morphology of the sludge were analyzed by SEM Hitachi S-3400N equipped with EDX. The sample was prepared into pellets by mounting it on standard pin-stubs with carbon tape. A brass carrier was then used to hold the sample. Under the operating condition at 15 kV, the SEM images were captured with magnification of 500X, 1000X, 2000X and 5000X. The elemental composition was then identified using the furnished EDX.

3.4.3 XRD

Structural analysis of the sludge was analyzed based on different peaks using X-ray diffractometer with the model XRD-6000 by Shimadzu. The sample was pressed tightly on a steel plate and making a smooth surface for a more precise analysis. The X-ray radiation employed was Cu $K\alpha$ radiations under the condition of 40 kV and 30 mA, scanning over two thetas (2θ) range from 10 to 85 degrees. The diffraction pattern was collected and recorded.

3.4.4 TGA

Analysis on the sample's thermal stability was conducted using Perkin Elmer STA8000 thermogravimetric analyzer. The sample was first placed in a small crucible above the balance to record its weight. After that, the sample was heated from 30 to 1000 °C, under inert air flow with a heating rate of 10 °C/minutes. The resulting changes in weight was recorded and plotted against temperature in order to quantify the percentage of volatile components present in the sample.

3.5 Sludge Digestion

Based on the information from characterization study, the digestion process was conducted in order to determine the total calcium (Ca) and aluminium (Al) concentration within the sludge. The total concentration is important to determine the leaching efficiency in the sludge treatment process. Based on the work of Sastre, et al. (2002), Aqua Regia digestion was adopted in an open vessel. To illustrate, 3 g of sludge was weighted into a 500 ml three neck round bottom flask. The pre-digestion step was completed at room temperature for 16 hours with the use of 37% HCl : 69 % HNO₃ mixture in a ratio of 3:1. After this, the suspension was digested at 130 °C under reflux condition for 2 hours. The suspension was then filtered and diluted to 100 ml with 0.5 M HNO₃. The diluted filtrate was stored in Schott laboratory bottle for analysis. The solid residues were dried, grinded and sieved to analyze its content through EDX.

3.6 Treatment of Sludge

The sludge sample was treated to reduce the concentration of Ca and Al metals. This step is essential for purifying the sludge and repurposing it for other applications. In this context, leaching process of the sludge was carried out with the use of 500 ml three neck round bottom flask. Moreover, a water-cooled coil condenser was installed to one of the necks to condense the evaporated liquid, while maintained a constant volume of the solution (Kurniawan, et al., 2022). Furthermore, a magnetic stirrer was applied to ensure well-mixing between the sludge and solution, whereas a heating mantle

was used to maintain uniform heating throughout the process. The experimental setup is illustrated in the Figure 3.2.

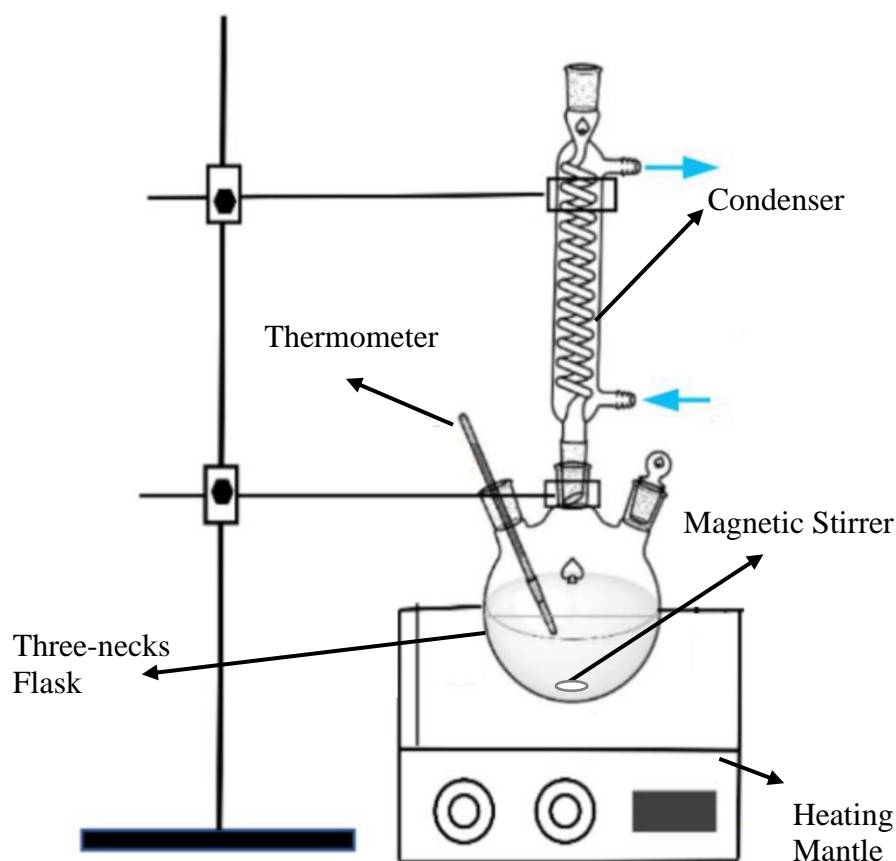


Figure 3.2: Experimental Setup of Acid Leaching (Guan, et al., 2022).

With a liquid-to-solid ratio (L/S) of 5:1, 3 g of sludge powder and 15 ml of 1.0 M H_2SO_4 were prepared. Once the temperature of the acid solution in the flask reached 30 °C, the sludge powder was added and the heating process was maintained for 30 minutes, with a constant rotational speed of 300 rpm. Furthermore, the temperature of the mixture was continuously monitored throughout the process using a thermometer. After the completion of the reaction, the mixture was transferred from the flask to the vacuum filter pump to separate the solid residues from the solution. The filtrate was collected for the subsequent analysis to determine the amount of Ca and Al being leached out. Meanwhile, the post-leached residues were washed with distilled water, dried, ground, sieved and kept in a sealed bag.

To conduct the parameter studies, the procedure was repeated with concentration of 0.3 and 0.5 M of H₂SO₄. Not only that, but each molar concentration (0.3, 0.5 and 1.0 M) was replicated with the use of HNO₃ and HCl, while other operating parameters kept constant. Following that, the optimal acid and its concentration in extracting Ca and Al were determined and employed. L/S ratio was varied across three different sets, including 3:1, 5:1 and 10:1, while keeping the weight of the solid sample at 3 g. After identifying the optimal L/S ratio, the effect of temperature on the leaching process was studied at 30, 50, 70, and 90 °C. Finally, the ideal temperature was utilized to conduct the leaching process for durations of 30, 60, 90, and 120 minutes to obtain the optimum result.

3.7 Sample Analysis

The filtrate from the digestion process and the leaching process was analyzed with Inductively Coupled Plasma Optical Emission Spectrometry (ICP-OES) model Perkin Elmer Optima 7000 to determine the Ca and Al concentration. Prior to carry out the analysis, a multi-element standard solution containing Ca and Al at a concentration of 500 mg/L was prepared using aluminium nitrate nonahydrate (Al(NO₃)₃·9H₂O) and calcium nitrate tetrahydrate (Ca(NO₃)₂·4H₂O) as precursors. About 0.295 g of Ca(NO₃)₂·4H₂O and 0.695 g of Al(NO₃)₃·9H₂O were dissolved with distilled water. After that, the solution was transferred into a 100 ml volumetric flask and distilled water was added until it reached the marked line on the flask. The standard solution was further diluted to 10, 20, 30, 40 and 50 mg/L to establish the calibration curve in the system.

The removal efficiency of both metals during the leaching process can be quantified by using Equation 3.1.

$$\text{Metal Removal Efficiency (\%)} = \left(\frac{C}{C_{total}} \right) \times 100 \quad (3.1)$$

where

C = leached Ca and Al content, mg/g

C_{total} = total Ca and Al in the solid sample, mg/g

CHAPTER 4

RESULTS AND DISCUSSION

4.1 Characterization Study of Raw Sludge

Characterization on raw rubber sludge was performed prior to acid leaching in order to identify the potential elements, as well as its association fraction.

4.1.1 FTIR

The functional groups attached on the sludge that collected from rubber industry were examined by using Fourier Transform-Infrared Spectroscopy (FTIR). Knowledge about the various functional groups present in the sludge is crucial, as inorganic substances or trace elements have a tendency to associate with these groups and form complexes (Arif Billah, Kuaanan Techato and Wirach Taweepreda, 2020). The spectrum of the sludge at a wavelength between 400 and 4000 cm^{-1} is shown in the Figure 4.1

First, a relatively strong absorption band at around 3278.02 cm^{-1} was identified, corresponding to the stretching mode of the hydroxyl group (O-H) (Kurniawati, et al., 2018). In this scenario, the presence of the O-H bond could potentially be attributed to the absorption of water molecules on the sample surface from the surrounding air during sample handling (Domínguez, et al., 2006).

According to Homkhiew, et al. (2018) and Emilia Agustina, Jefri Sirait and Silalahi (2017), one of the primary pollutants found in the rubber sludge waste is latex. In this context, dominant characteristic peaks associated with cis-1,4-polyisoprene compound, a constituent of natural rubber, were observed at 2960 cm^{-1} (CH_3 asymmetric stretching), 2920.19 cm^{-1} (CH_2 asymmetric stretching), 2853 cm^{-1} (CH_2 symmetric stretching), 1632.87 cm^{-1} (C=C stretching) and also 1408.68 cm^{-1} (C-H deformation). The results were aligned with the findings reported in the studies by Valera-Zaragoza, et al. (2014) and Rahmah, et al. (2019). Besides, these functional groups might also originate from organic compounds, such as carbohydrates, lipids and proteins.

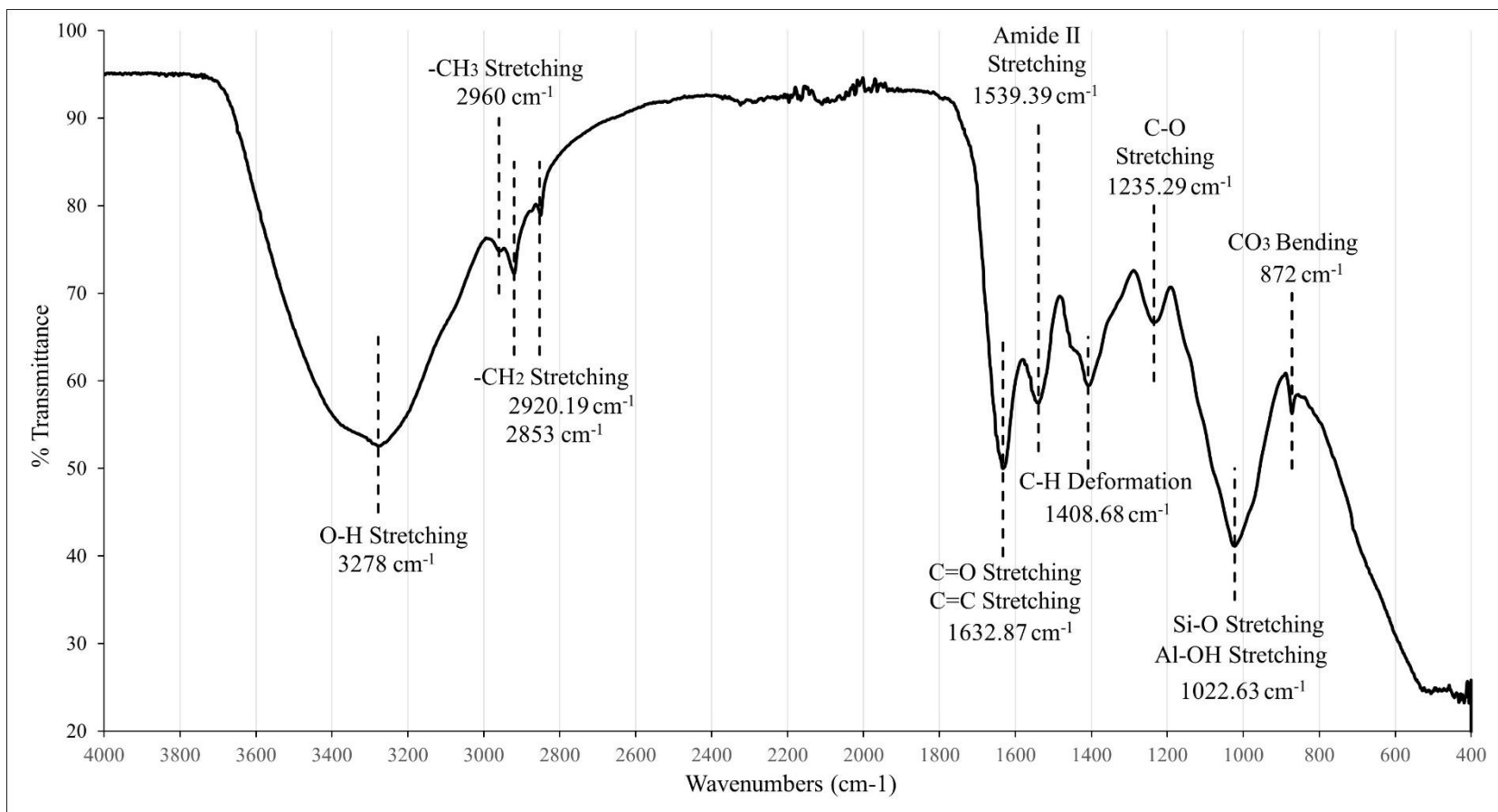


Figure 4.1: FTIR Spectrum of Raw Rubber Sludge.

Non-isoprene compounds, such as amide, silica and carbonate groups, were also observed in the sample. The presence of these compounds could originate from additives, including vulcanizing agents, plasticizers, softeners, fillers, antioxidants, stabilizers and other chemical compounds that introduced during rubber product manufacturing (Lovato, et al., 2023). In terms of the amide II (N-H) stretching at wavenumber 1539.39 cm^{-1} , it could possibly come from extractable proteins, which are natural components present in natural rubber latex. To elucidate, these proteins tend to migrate to the surface of the rubber-product during drying and heat vulcanization processes (Perrella and Gaspari, 2002). In order to eliminate these surface proteins, the leaching approach was employed during rubber product processing, resulting in their presence as pollutants in the sludge.

In addition, Kurniawati, et al. (2018) stated that the peak at 1632.87 cm^{-1} was also associated with the stretching vibration mode of the C=O bond. Besides, the peak value at 1235.29 cm^{-1} signified the stretching mode of the C-O bond, whereas the small peak at around 872 cm^{-1} was assigned to the out-of-plane bending mode of the carbonate group. As indicated in the study by Molla, et al. (2022), these vibrational bands can be attributed to the CO_3^{2-} group in calcite. On top of that, the band at 1022.63 cm^{-1} was indicative of the stretching vibration of the Si-O bond, possibly due to the presence of silica (SiO_2), or the characteristic bending of Al-OH (Veerasingam and Venkatachalapathy, 2014; Azdarpour, et al., 2015).

4.1.2 SEM-EDX

Scanning Electron Microscopy (SEM) analysis was conducted to assess the surface morphology of the sludge. The SEM images of the raw sludge from the rubber industry are presented in Figure 4.2 with Figure 4.2 (a), Figure 4.2(b) and (c) illustrating the raw sludge at magnifications of 500X, 2000X, and 5000X, respectively.

From the SEM micrographs, it was observed that there was no well-defined crystalline structure on the sludge surface, indicating its amorphous nature. This observation aligned with the findings by Awab, Paramalingam and Mohd Yusoff (2012) conducted on water treatment sludge. According to Haynes and Zhou (2015), sludge typically remains in an amorphous state due

to the interaction between the inorganic and organic substances during the wastewater treatment process, which eventually prevents its crystallization. Besides, the sludge surface was slightly porous and irregular, mainly due to the heterogeneous distribution of particles. On top of that, Czechowska-Kosacka (2019) suggested that the small irregular-shaped clusters on the sludge surface were attributed to the presence of minerals. Additionally, the sludge exhibited a few microcracks. The formation of microcracks could be induced by the sample preparation technique prior conducting the analysis. According to Amin and Salihoğlu (2021), the drying process could lead to the development of microcracks on the sludge surface due to shrinkage.

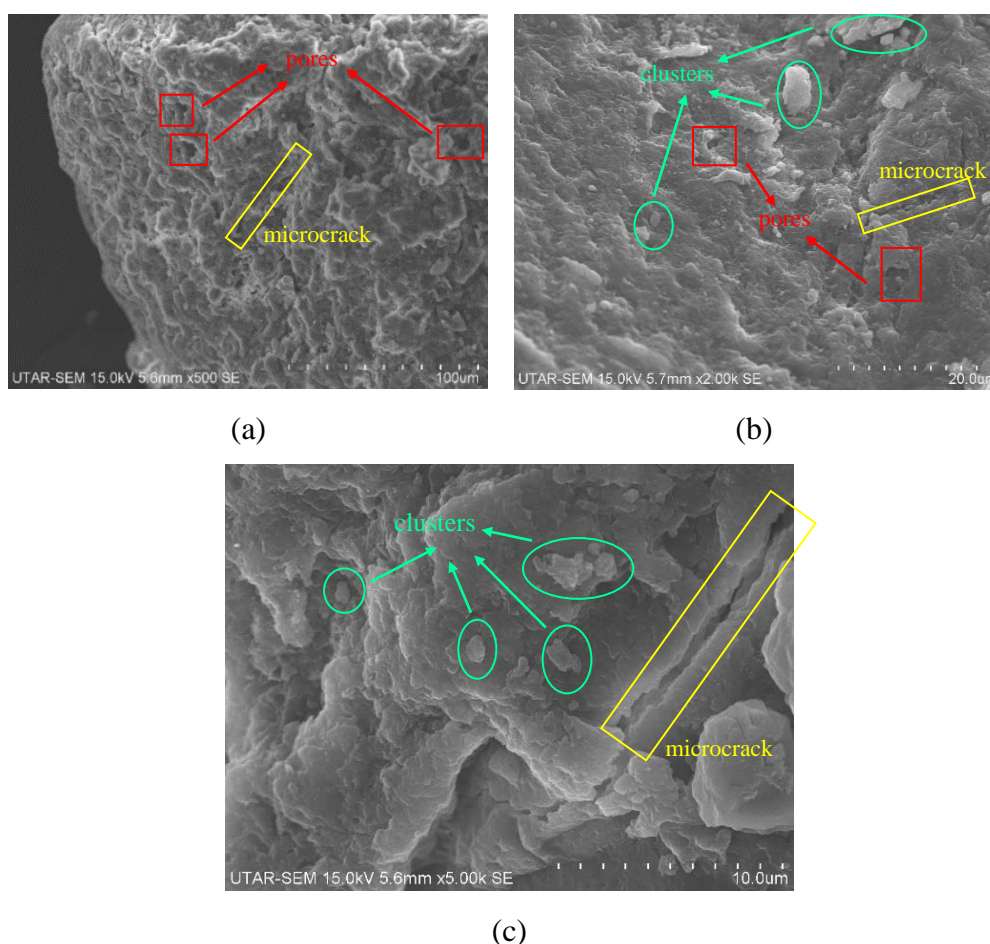


Figure 4.2: SEM Images of Raw Rubber Sludge at Magnification of (a) 500X, (b) 2000X and (c) 5000X.

On top of that, Energy Dispersive X-Ray (EDX) analysis was performed to investigate the elemental distribution on the surface of the sludge.

Table 4.1 summarizes the major elements that being measured in the analysis. It was confirmed that the sludge surface mostly contained the elements oxygen (O) - 27.10 %, carbon (C) - 18.05 %, calcium (Ca) - 19.91 %, aluminium (Al) - 12.52 % and silicon (Si) - 8.0 %. As stated, the composition of the sludge is affected by the pollution load, the nature of the wastewater treated and the methods of treatment employed. Therefore, the availability of these elements was discussed in relation to these aspects.

Table 4.1: Elemental Composition of Sludge from EDX.

Elements	Percentage (wt%)
Carbon (C)	18.05
Oxygen (O)	27.10
Aluminium (Al)	12.52
Silicon (Si)	8.00
Calcium (Ca)	19.91
Sodium (Na)	1.80
Phosphorus (P)	4.09
Sulfur (S)	3.53
Chlorine (Cl)	1.75
Potassium (K)	3.53

The presence of C and O as the organic elements was notable, owing to their roles as key building blocks of chemical compounds. To elucidate, the significant proportion of oxygen could be attributed to the bound oxygen found in organic substances in the sludge, or the dissolved oxygen from the atmosphere and the aerated wastewater treatment process.

In addition, the source of Ca element was largely be attributed to the additives introduced during the fabrication of rubber products. For instance, during the stage of coagulant dipping, formers were soaked in a coagulant bath containing calcium nitrate and calcium carbonate. Calcium nitrate helps to ensure good adherence of latex to the former, whereas calcium carbonate functions as an anti-tack agent to facilitate the detachment of rubber products

from the mold. Not only that, but calcium carbonate is used as low-cost non-reinforcing fillers to enhance the mechanical properties of rubber products.

Besides, the presence of Al element was originated from the additives introduced during the fabrication of rubber products, as well as the chemicals used during wastewater treatment. To highlight, aluminium-based compounds act as crosslinkers for the vulcanization effect. In terms of wastewater treatment, alum is used as coagulants to remove suspended solids, particularly the fine dispersed latex particles (Perapong and Surajit, 2006). For the Si, it is typically applied as reinforcing fillers, which can enhance the rubber abrasive properties even in small amounts (Amdur, 2019).

Other elements, including phosphorus, sulfur, potassium, sodium and chlorine were detected in trace quantities, which could be explained by the contaminants encountered during sludge handling, as well as the small amount of chemicals used during the processing of rubber products and wastewater treatment.

4.1.3 XRD

The possible crystalline phase within the sludge from the rubber product industry was evaluated through X-ray Diffraction (XRD) analysis in the range from 10 to 85 degrees. The diffraction peaks were compared with the RRUFF database. The results are depicted in Figure 4.3.

The identified peaks were predominantly made up of calcite (CaCO_3) and gibbsite ($\text{Al}(\text{OH})_3$). However, only CaCO_3 was mainly observable, with detected peaks at 23.12, 29.46, 31.48, 36.06, 39.50, 43.22, 47.18, 47.52, 48.56, 56.58, 57.46, 60.70 and 70.26°. Apart from that, in terms of $\text{Al}(\text{OH})_3$, it was mainly identified at 19.1, 20.06, 28.36, 38.34, 50.78 and 64.24°. Besides, a broad peak at around 17° suggested the existence of amorphous silica (SiO_2). These prominent peaks were aligned with the FTIR and EDX results. To elucidate, due to the high concentration of Ca compared with other elements, peaks from other substances could hardly be observed against this background. Nevertheless, the presence of the major elements could still be confirmed by considering the FTIR spectrum and EDX analysis.

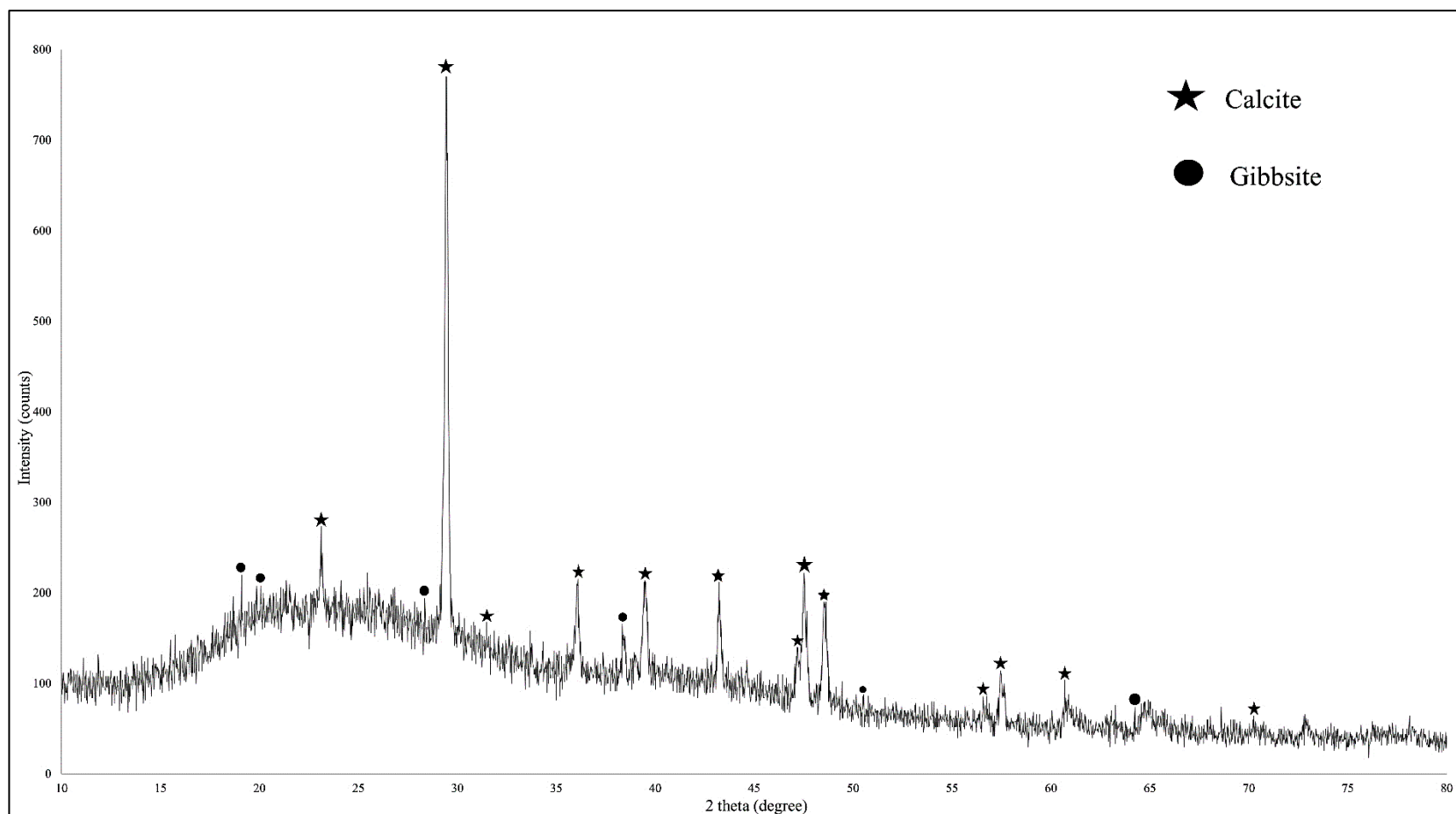


Figure 4.3: XRD of Raw Rubber Sludge.

4.1.4 TGA

Thermogravimetric Analysis (TGA) was performed under a heating rate of 10 °C/min from 30 to 1000 °C under an inert atmosphere to study the thermal decomposition behavior of the sludge. Figure 4.4 displays the TGA curve to assess the weight change of rubber sludge upon heating.

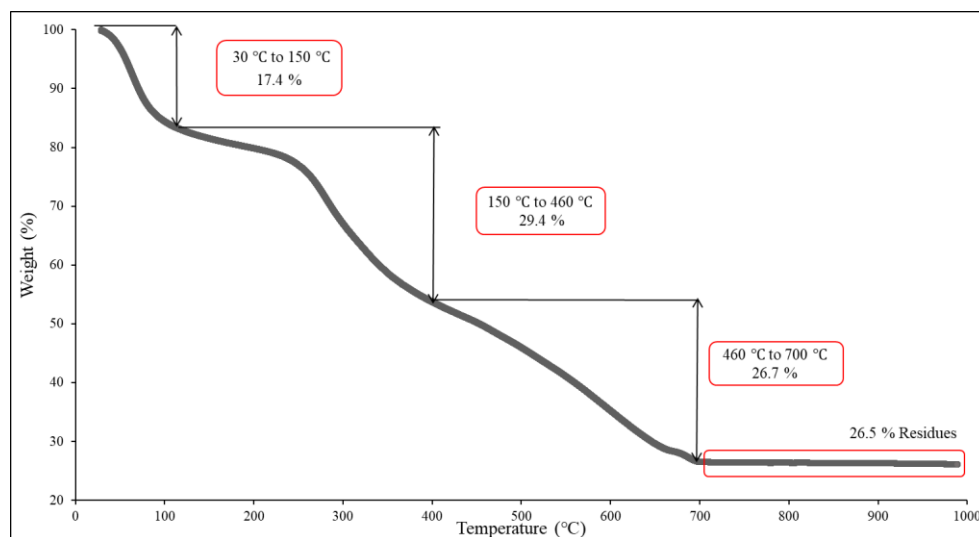


Figure 4.4: TGA Curve of Raw Rubber Sludge.

It was evident from the TGA curve that the decomposition of the sludge occurred in three distinct stages. During the initial phase from 30 to 150 °C, there was an approximately 17.4 % weight loss due to dehydration. To highlight, the mass loss of up to 100 °C was due to the evaporation of residual free water that remained after the drying process, or physically reabsorbed moisture from the atmosphere. In addition, interstitial water occupying the pore spaces in the sludge was eliminated starting from a temperature of 100 °C (Uttara Mahapatra, et al., 2021).

The second stage, spanning the temperature range of 150 to 460 °C, a weight loss of 29.4 % was observed. The dramatic weight loss within this range was associated with the volatilization of organic substances, comprising carbohydrates, proteins and lipids. On top of that, it was asserted by Onchoke, Franclemont and Weatherford (2018) that the decomposition of weaker hydroxyl bond occurred as well in this phase, between 210 and 310 °C. The study by Shamaki, Adu-Amankwah and Black (2021) found that the dehydroxylation of $\text{Al}(\text{OH})_3$ to alumina occurred at 200 °C, provided

additional support for this claim. In the studies of Silva, et al. (2020) and Tertyshnaya, et al. (2022), degradation of natural rubber occurred at 374 and 350 °C, respectively. Accordingly, it was proposed that the disintegration of the latex residues within the sludge had occurred at this stage.

The third slope in the temperature range of 460 to 700 °C revealed a total weight loss of 26.7 %. This phenomenon was attributed to the disintegration of inorganic species like CaCO_3 to form calcium oxide and carbon dioxide gas (Onchoke, Franclemont and Weatherford, 2018). Along with this, at around 579 °C, a transition from α -quartz to β -quartz, which has the potential to remain stable up to 1000 °C, had taken place (Shamaki, Adu-Amankwah and Black, 2021). Furthermore, a residue of about 26.5 % was identified with the trend showing a plateau starting from 700 °C.

In summary, the sludge displayed a relatively balanced distribution of organic and inorganic substances, as evidenced by the closely comparable weight loss observed at the second and third stages.

4.2 Acid Digestion of Sludge

In order to investigate the total concentration of Ca and Al metals using Inductively Coupled Plasma - Optical Emission Spectrometry (ICP-OES), the rubber sludge was digested using Aqua Regia, a concentrated mixture of HNO_3 and HCl with a volume ratio of 1:3. To mention, Ca and Al were chosen for concentration evaluation due to their higher proportion on the surface compared to other metals. Specifically, Ca accounted for 19.91 % and Al for 12.52 %, as determined through the characterization study. Furthermore, it should be emphasized that EDX merely provided the distribution of elements on the surface, thereby ICP-OES analysis was crucial to obtain more precise qualitative data on the total metal content (Michalak, et al., 2014).

Through multi-elemental analysis, Ca was found to be present at a concentration of 71.88 mg/g of sludge, whereas Al was identified at 47.47 mg/g of sludge. The result stayed in agreement with the previous EDX analysis result. This Ca / Al ratio was closely comparable, at 1.59 for the EDX technique and 1.51 for the ICP-OES analysis. Besides, EDX examination was performed on the residues that remained undigested, as shown in Appendix B. The result indicated that Ca had fully dissolved, while the amount of Al on the

surface of sludge was only 0.09 wt. %. This further validated the reliability of the data concerning the total metals concentration in the sludge.

4.3 Parameter Studies in Acid Leaching of Sludge

Acid leaching is one of the methods used to treat sludge containing high concentration of Ca and Al metals. It was selected due to its high leaching rate and ease of execution. Metals embedded in the sludge particles are dissociated and transformed into their ionic state by hydrogen ions in the acid. The ionic metal species are then released into the solution, leading to their presence in the leachate (Gunarathne, et al., 2022). Various parameters can impact the efficiency of metal extraction, including the types and concentration of acids used, leaching temperature, liquid-to-solid ratio (L/S), and the duration of the treatment process. Each of these parameters will be examined in the following subsections.

4.3.1 Effect of Types of Acids and its Concentration

The types of acids, along with its concentration significantly contributed to the extraction performance of Ca and Al. To investigate the effect of different types of extractants with varying molar concentration, hydrochloric acid (HCl), sulfuric acid (H_2SO_4), and nitric acid (HNO_3) at 0.3, 0.5 and 1.0 M were used as the extracting agents. The extraction rates for Ca and Al are illustrated in Figure 4.5 (a) and Figure 4.5(b), respectively.

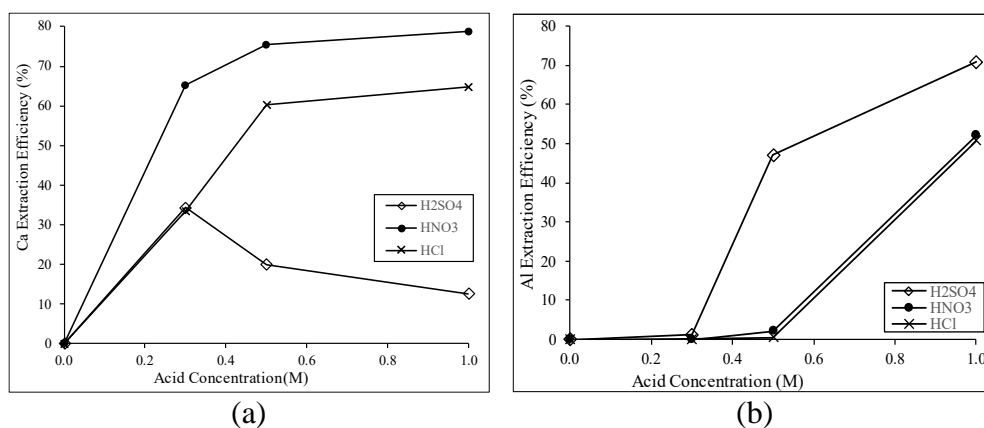
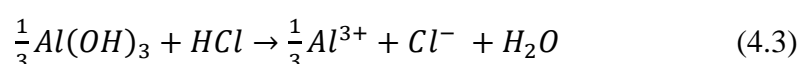
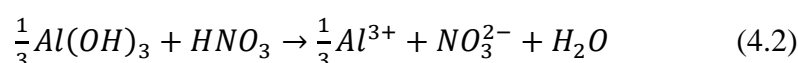
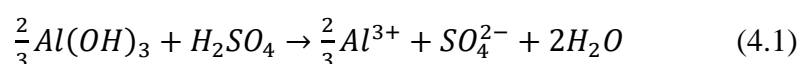


Figure 4.5: Extraction Efficiency using Different Acids and Concentration on (a) Ca and (b) Al.

In terms of Ca extraction efficiency, Figure 4.5 (a) shows that both HNO₃ and HCl were able to extract a significant amount of Ca. However, H₂SO₄ was deemed unsuitable for removing Ca from the sludge, as indicated by a declining trend in extraction efficiency. This could be attributed to the reaction between the dissociated Ca²⁺ ions and H₂SO₄, resulting in the formation of calcium sulfate (CaSO₄) (Lee, et al., 2021). To elucidate, CaSO₄, which is low solubility in nature, was believed to precipitate on the sludge surface rather than dissolving into the solution.

On the contrary, when H₂SO₄ was utilized to remove Al from the sludge, it achieved the highest extraction efficiency among the acids, followed by HNO₃ and HCl. To further elaborate, Al may exist in the hydroxide form, as identified in the characterization study. Equation 4.1, 4.2 and 4.3 were used to indicate the dissolution of Al by acid solutions:



Based on stoichiometry basic, the reactions revealed that one mole of H₂SO₄ could dissolve two-third of an Al³⁺ ion, whereas one mole of HNO₃ and HCl could only dissociate one-third of an Al³⁺ ion. Additionally, H₂SO₄ generates twice as many hydrogen ions at the same concentration as HNO₃ and HCl. Therefore, it was suggested that the Al leaching rate using H₂SO₄ was significantly more effective. These findings corresponded to the study by Widi Astuti, et al. (2016) on nickel dissolution.

On top of that, it was shown that increasing the acid concentration contributed to the extraction rate of both Ca and Al. As the acid concentration increased from 0.3 to 1.0 M, the rate of Ca removal rose from 65.3 to 78.8 % when using HNO₃. Similarly, the leaching rate of Al raised from 33.4 to 64.9 % with the used of HCl. On the other hand, the efficiency of Ca removal in H₂SO₄ decreased from 33.4 to 12.5 %. It could be explained by the fact that

more sulfate ions and supersaturation of Ca eventually facilitated the precipitation of CaSO_4 (Nayak and Panda, 2010).

Additionally, poor extraction efficiency was recorded when using 0.3 M acid to remove Al, ranging from 0.1 to 1.2 % for all three acids. Along with that, H_2SO_4 demonstrated a notable escalate, from 47.0 % at 0.5 M to 70.7 % at 1.0 M. Nevertheless, both HNO_3 and HCl showed a gradual increase up to 0.5 M, eventually reaching 52.06 and 50.67 %, respectively, at 1.0 M. Overall, it was apparent that the Al extraction efficiency was lower compared to Ca. According to He, et al. (2021), this discrepancy could be linked to the higher valence state of Al^{3+} ions, which resulted in a higher charged density than Ca. Thence, the absorption ability of sludge particles to Al was stronger, inevitably affecting the kinetics of the Al leaching process.

In summary, the highest extraction rate for Ca was attained at 1.0 M of HNO_3 , while the optimal leaching rate for Al was 1.0 M of H_2SO_4 . However, considering that the formation of CaSO_4 precipitates can lead to the accumulation of insoluble product layer on sludge particles, thereby blocking pore channels and impeding the diffusion of hydrogen ions into the interior of the sludge particles (Tao, et al., 2021). This may impact the leachability of Al in subsequent parameter studies. Therefore, 1.0 M of HNO_3 was selected as the leachant for both Ca and Al.

4.3.2 Effect of Liquid-to-Solid Ratio

To explore the effect of liquid-to-solid ratio (L/S) on the leaching of Ca and Al, it was manipulated at 3:1, 5:1 and 10:1. The graph depicting extraction efficiency against the L/S ratio 30 °C for 30 minutes with 1.0 M of HNO_3 is plotted in Figure 4.6. A positive relationship between the leaching rate and the L/S ratio was observed.

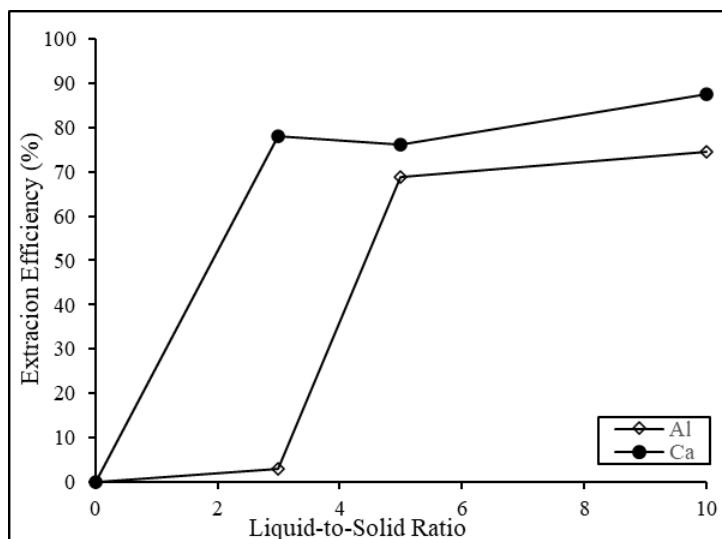


Figure 4.6: Effect of L/S Ratio on Extraction Efficiency of Ca and Al.

With an increase in the L/S ratio, the leaching efficiency of Ca improved from 77.93 to 87.64 %, and that of Al increased from 3.02 to 74.41 %. To illustrate, the lower leachability of both metals at a ratio of 3:1 was due to the limited amount of HNO_3 available for complete contact with the sludge particles. This, in turn, reduced the effective surface area for interaction between the sludge particles and extractant, leading to incomplete dissolution of Ca and Al. Besides, lumps with certain stickiness were easily formed when the L/S ratio was low. These clumps eventually impeded the contact of Ca and Al with HNO_3 (Wang, et al., 2020). As a consequence, there was a lower extraction efficiency as the mass transfer rate was slower due to diffusion resistance.

In contrast, a higher L/S ratio of 10:1 had accelerated the leaching process, as there were more hydrogen ions available to diffuse into the internal pores or unreacted zone of the sludge and displace the metals. Hence, more metal ions were formed and practically leached, which led to the optimal results. Nevertheless, a slight decrease in Ca extraction, around 1.7 % was observed at the ratio of 5:1. It might be attributed to the slight saturation of the metal ions around the sludge particles, resulting in a diffusion limitation of these ions to into bulk solution. To summarize, the optimum L/S ratio for removing both Ca and Al was found to be 10:1.

4.3.3 Effect of Temperature

The role of temperature in affecting the leaching rate of Ca and Al was examined by varying the temperature at 30, 50, 70 and 90 °C, using 1.0 M HNO₃, 10:1 L/S ratio over 30 minutes. Figure 4.7 reveals the resulting yield with each temperature increment.

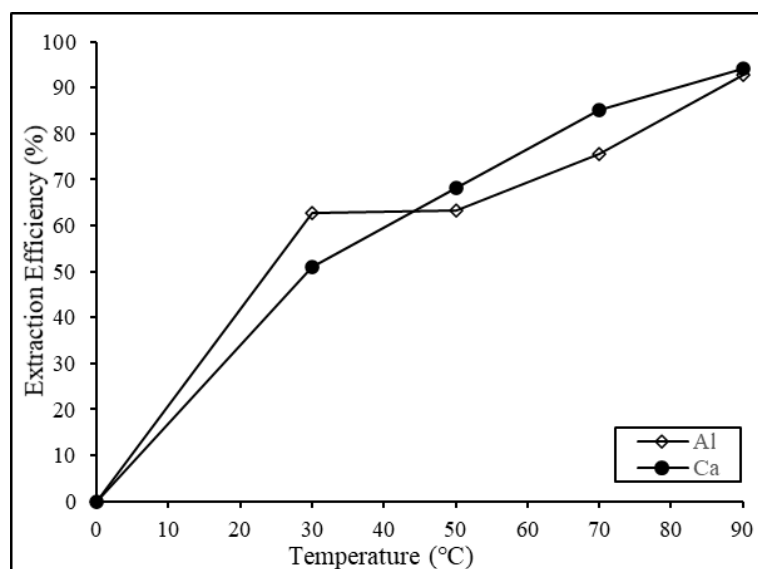


Figure 4.7: Effect of Temperature on Extraction Efficiency of Ca and Al.

According to the results, the leaching efficiency of Ca exhibited a consistent upward trend, rising from 51.04 % at 30 °C to 94.14 % at 90 °C. For Al, a yield of 62.82 % was achieved at 30 °C, with a slight increase to 63.20 % at 50 °C, and finally a notable improvement to 92.82 % when the temperature further rose to 90 °C. This phenomenon could be explained in terms of the mass transfer process, where the kinetic energy of hydrogen ions in HNO₃ increased during high-temperature leaching. This sped up the diffusion rate of ions through the pores of sludge particles, aiding in the dissolution of Ca and Al (Alkan, et al., 2018). In view of the aspect of reaction, the speed of the molecular motion and collision frequency between the metal compounds in sludge particles and hydrogen ions enhanced in response to temperature (Wang, et al., 2019). This subsequently induced the dissolution of Al and Ca, leading to their presence in ionic form. Additionally, Chi, et al. (2006) and He, et al. (2021) suggested that the leaching process is endothermic. Therefore, higher temperature encouraged the dissolution of Ca and Al as more energy

was provided to break the associated bonds. Nevertheless, the study was limited to 90 °C was based on the observation that this temperature resulted sufficient leaching efficiency to achieve the desired outcomes. Additionally, conducting experiments at higher temperatures could introduce safety concerns. To conclude, the temperature of 90 °C ensured a balance between effective results and safety considerations.

4.3.4 Effect of Duration

To investigate the impact of time on the extraction efficiency of Al and Ca throughout the leaching process, the leachate was collected at intervals of 30 minutes, until reaching 120 minutes. Figure 4.8 provides an illustration of the outcomes, under the conditions of 1.0 M of HNO₃, 10:1 L/S ratio at 90 °C.

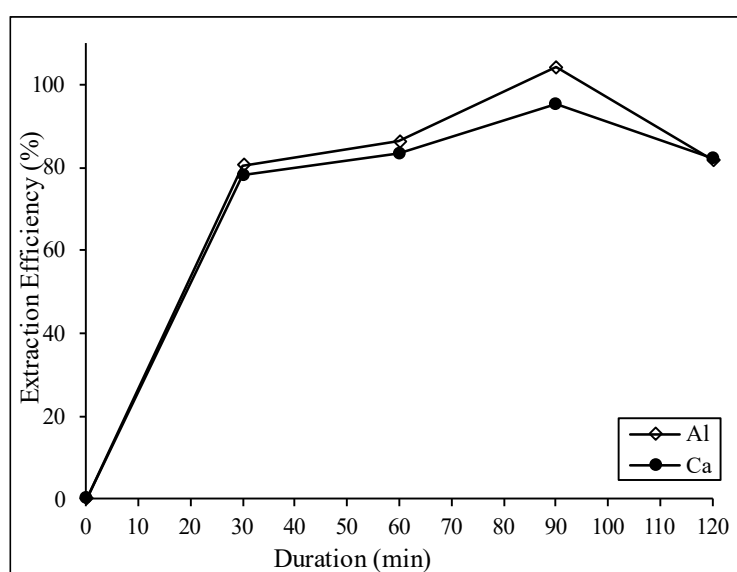


Figure 4.8: Effect of Duration on Extraction Efficiency of Ca and Al.

Both curves exhibited a similar trend. Both Ca and Al extraction efficiency augmented with the increased of leaching period up to 30 minutes, but not markedly in the subsequent period of 30 to 60 minutes. However, when the leaching period was extended to 90 minutes, the extraction efficiency increased again, reaching its peak rate of 95.21 % for Ca and 100 % for Al. Following that, both extraction efficiency of Ca and Al dropped to 82.22 and 81.74 %, respectively.

This phenomenon could be explained in several phases. In the initial phase, the exponential increase in leaching efficiency of Ca and Al was attributed to the presence of readily available hydrogen ions, as well as Ca and Al compounds on the sludge surface, which prompted a rapid dissolution reaction at the solid-liquid interface. At the second stage from 30 minutes to 60 minutes, most of the surface metals had already been leached, leaving behind an unreacted zone containing tightly packed Al and Ca compounds, which caused a limited growth in the leaching rate. On top of that, further extending the leaching duration to 90 minutes enhanced the diffusion of hydrogen ions into the interior part of sludge particles. Meanwhile, there was also a longer contact between the metals and hydrogen ions, which facilitating the dissolution reaction of Ca and Al into the solution (Cao, et al., 2018). However, a prolonged leaching duration had a negative effect on extracting Ca and Al. It may be due to the reabsorption of dissolved metal ions onto the sludge surface, ultimately reducing their concentration in the aqueous solution.

In overall, the optimal result in the leaching study was observed at 1.0 M HNO₃, 10:1 L/S ratio, 90 °C and 90 minutes.

4.4 Post-Leached Residues Studies

The post-leached solid residues, including the residues from acid selection studies (RAS) mainly focused on H₂SO₄ to prove the precipitation of CaSO₄, as well as the residues from the optimal results (ROR), were dried and analyzed in the following sections.

4.4.1 Physical Appearances

The primary focus of this section is to examine the physical appearance of the RAS and ROR, as depict in the Figure 4.9 (a) and (b), respectively. To clarify, the raw sludge, which was a type of activated sludge, appeared brown in colour due to mixing with microbial aggregates. In this context, it was believed that the removal of Ca and Al had no noticeable effect on the colour, as the ROR retained its brown colour. Nevertheless, it was clearly observed that the residues became pale, and white in colour when the sludge was leached with H₂SO₄. This change in colour was mostly associated with the precipitation of Ca in the form of CaSO₄, as discussed previously. This sulfate

compound was white and sparingly soluble in nature, contributing to the visually lighter appearance of the residues.

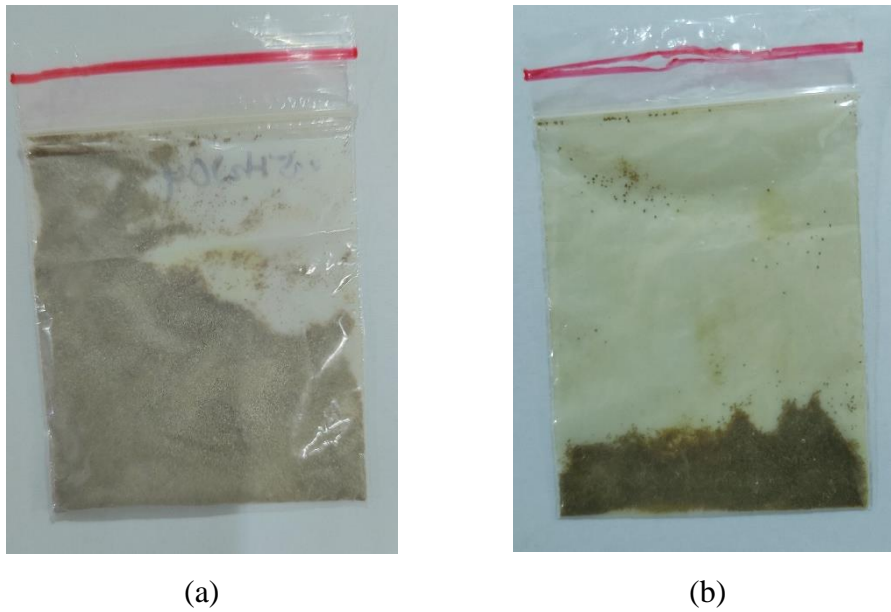


Figure 4.9: Physical Appearance of (a) RAS and (b) ROR.

4.4.2 SEM

In terms of SEM examination, Figure 4.10 (a) and (b) display the morphological observation of RAS treated with H_2SO_4 , as well as the ROR.

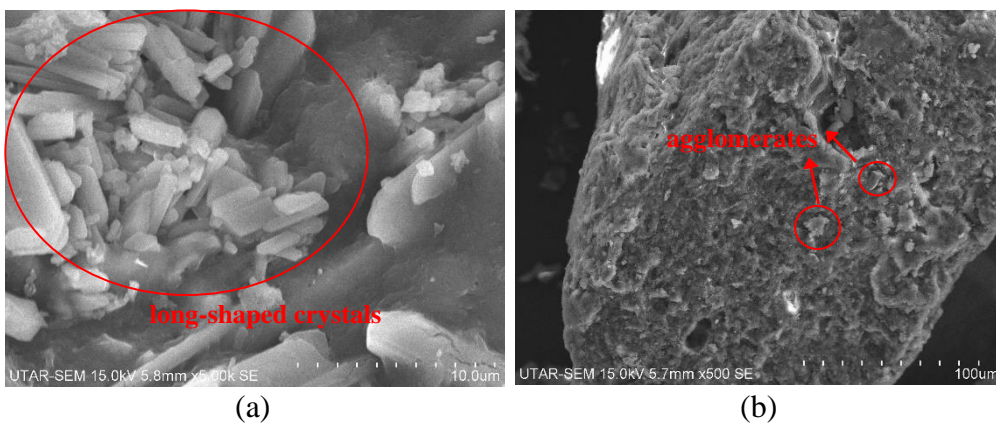


Figure 4.10: Morphology of the (a) RAS with H_2SO_4 and (b) ROR.

Long-shaped crystals, which were absent in the raw sludge, were observed on the surface of post-leached sludge treated with H_2SO_4 , as shown in Figure 4.10 (a). This morphological observation aligned with research conducted by Havlik, et al. (2019), providing additional confirmation of the

build-up of CaSO_4 on the surface of the sludge. If H_2SO_4 continued to be utilized in the leaching process, this may eventually impede the treatment process for extracting Al. Moreover, the ROR revealed a surface that was coarser and more porous, which caused by the acid attack during the leaching process (Nayak and Panda, 2010). However, the residues still consisted of a few agglomerates, indicating that some impurities were not removed.

4.4.3 FTIR

The distinctive characteristics transmittance bands in RAS and ROR are illustrated in Figure 4.11. In order to prove the existence of CaSO_4 precipitates, its fundamental peaks were identified. To illustrate, the peak at 3524.70 and 3399.73 cm^{-1} were ascribed to the stretching of the hydroxyl group (Fernández-Carrasco, et al., 2012). Based on the work of Nicoara, et al. (2023), the band at 3524.70 cm^{-1} corresponded to the water molecules, while the band of CaSO_4 was at the value of 3399.73 cm^{-1} . Moreover, the peaks at 1620.12 and 1529.30 cm^{-1} represented strong -OH bending. It was inferred that the CaSO_4 precipitates were not anhydrite or bassanite, but rather gypsum, which is the hydrated form. On top of that, the observed peaks at 1100, 665.02 and 598.62 cm^{-1} were due to the S-O stretching, as well as the in and out-of-plane bending of the sulfate group (Kamaraj, et al., 2017).

Apart from that, it was evident that the peaks related to the carbonate group in the raw sludge had diminished. As highlighted in Figure 4.11, the transmittance intensity of the hydroxyl group, as well as the Si-O and Al-OH had been reduced compared to the raw sludge, which signified the breakage of these associated bonds. Furthermore, the newly emerging absorption bands at 1453.42 and 1377.55 cm^{-1} were the result of - CH_3 and C-H group bending (Awale, et al., 2018). On top of that, the peak at 1161.86 cm^{-1} was caused by the antisymmetric stretch vibrations of Al-O-Si or Si-O-Si (Hou, et al., 2022).

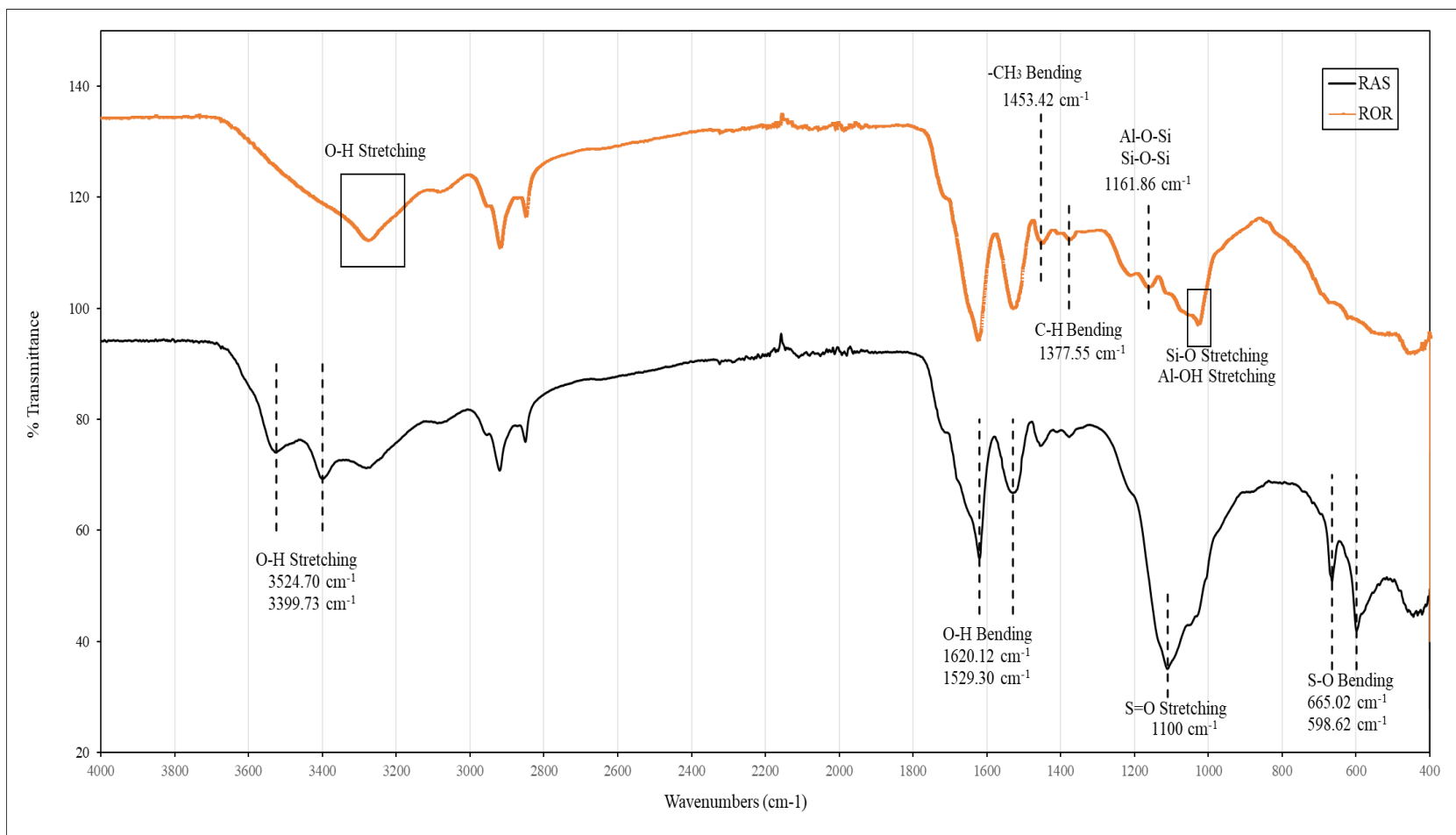


Figure 4.11: FTIR Spectra of RAS with H₂SO₄ and ROR.

4.4.4 XRD

The mineralogical analysis from the RAS and ROR are shown in Figure 4.12, It was noticeable that in the post-leached residue treated with H_2SO_4 , RAS showed sharp peaks at angles of 12.08, 21.16, 23.86, 29.56, 35.00, 36.34, 37.08 and 43.78°. The results from the RRUFF database and the research of Azdarpour, et al. (2015) indicated that these peaks were analogous to gypsum. The results further confirmed the precipitation of Ca in H_2SO_4 .

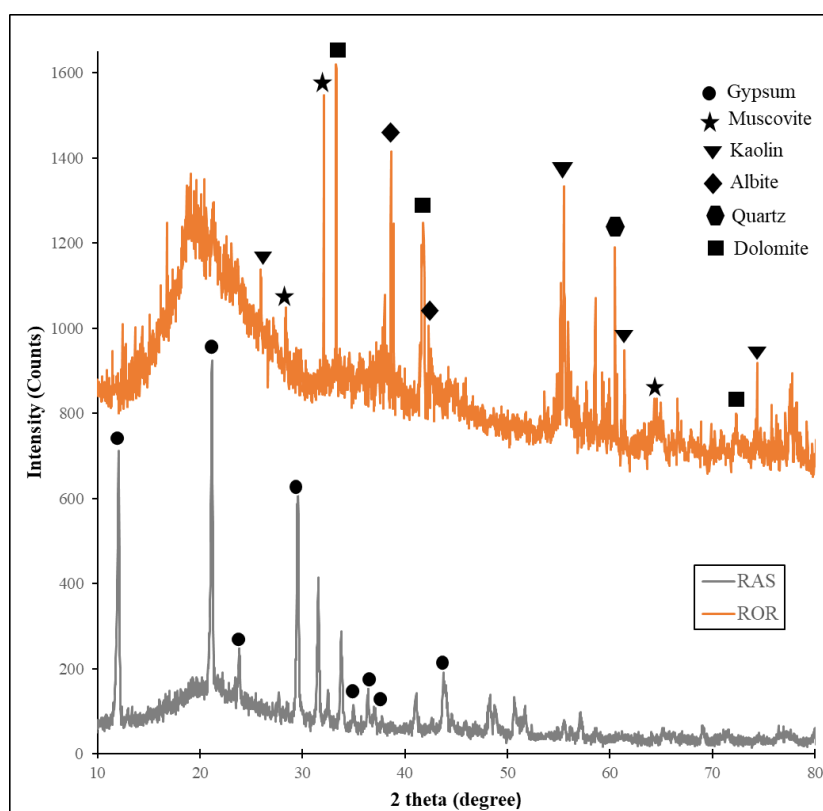


Figure 4.12: Diffraction Peaks of RAS with H_2SO_4 and ROR.

On the other hand, ROR possessed a distinct pattern with the raw sludge, as presented in Figure 4.3 above. To elucidate, the peaks of $CaCO_3$ and $Al(OH)_3$ that were identified in the raw sludge were suppressed, proving their dissolution during the HNO_3 leaching process. The newly emerging sharp peaks were believed to be constituted by quartz, aluminosilicate minerals and dolomite, which were previously unknown in the raw sludge due to their low concentration.

Firstly, the presence of quartz was detected at $2\theta = 60.5^\circ$. Besides, peaks of aluminosilicate minerals, including muscovite at $2\theta = 28.30, 32.10$

and 65.00° , as well as albite at 38.66 and 42.32° . These findings of minerals might come from the environmental contamination during sludge handling. Additionally, peaks at 25.96 , 55.50 , 61.44 and 74.38° were identified as kaolin. According to Nadesan (2018), this compound is typically added to the nitrile rubber compounds as a filler to reduce the possibility of surface defects. Besides, the characteristic peaks of dolomite were evaluated at $2\theta = 33.32$, 41.80 , 66.58 , and 72.36° . Due to highly complicated structure of these crystalline compounds, their solubility is substantially lower and may require more critical conditions to dissociate. In this regard, Gunarathne, et al. (2022) stated that the metals encapsulated in crystalline silica assemblages are more resistant to acid leaching due the extreme stability of Si-O bonds. Furthermore, a wide peak which in the range of 15 to 30° corresponded to the amorphous silica.

4.5 Potential for Reutilization

The discussion will analyze the feasibility of reuse for the solid residues and the leachate. Firstly, the apparent increase in roughness and pore volume, as well as the primarily carbon-based post-leached residues with HNO_3 enable them to be repurposed as low-cost adsorbents to remove a wide range of pollutants, such as dyes or heavy metals (Smith, et al., 2009). In this context, the elemental composition of the post-leached residues with HNO_3 is demonstrated in Appendix E. Additionally, a high carbon and low oxygen content in the residues can provide an increase in the higher heating value (HHV), indicating its feasibility as a source of energy, such as bio-oil (Supaporn, et al., 2019). On top of that, owing to their mostly organic composition, with up to 68 % of carbon, the sludge residues are believed to improve the condition of particle aggregation when incorporated into the soil. This results in a decrease in density and an improvement of the macro porosity, allowing the soil better aeration and water retention capacity (Campos, et al., 2019). To elucidate, since most heavy metals have been leached out during the treatment process, it might reduce the possibility of these pollutants leaking into the environment when applied to soil.

As for the leachate, which mainly consists of Al ions and Ca ions, they can be extracted through various techniques, such as chemical

precipitation, ion-exchange, solvent extraction and crystallization process. Hou, et al. (2022) proposed that the leachate can be subjected to concentrated crystallization in order to obtain nitrate crystals. In this context, calcium nitrate can be further treated for use as fertilizer or reused in the rubber industry for latex coagulation, promoting a closed-loop circular economy. Aluminium nitrate can also be used in tanning leather. Accordingly, the authors suggested that additional decomposition of the nitrate crystals can result in the formation of metal oxides. At the same time, the gases generated can be absorbed by water to regenerate it as nitric acid.

CHAPTER 5

CONCLUSIONS AND RECOMMENDATIONS

5.1 Conclusions

To conclude, the characterization of sludge collected from the rubber industry, as well as the utilization of acids in leaching aluminium and calcium from the sludge had been explored. The FTIR spectrum in the raw sludge illustrated the stretching mode of hydroxyl group due to the absorption of moisture, alkanes and alkenes group, believed to come from the isoprene compound, as well as the presence of silica, carbonate and amide groups, due to the additives introduced during rubber products manufacturing. Furthermore, the surface morphology of the raw rubber sludge was found to be amorphous, porous and irregular. Meanwhile, according to EDX analysis, Ca and Al were the most abundant elements on the sludge surface. Along with that, XRD analysis further confirmed the existence of Ca and Al, in the form of calcite and gibbsite. Based on the TGA results, the thermal stability of the sludge exhibited three distinct stages of decomposition: the first stage from 30 to 150 °C involved the dehydration process, followed by volatilization of organic substances, dehydroxylation of weak hydroxyl compound, and disintegration of latex residues in the sludge from 150 to 460 °C during the second stage, meanwhile decomposition of carbonate compound at the third phase up to 700 °C. Furthermore, since the weight loss in the second and third stages was nearly equal, the distribution of organic and inorganic substances in the raw rubber sludge was substantially equilibrium.

The treatment process to remove Ca and Al was done by acid leaching due to its speedy and simplicity in operation. Various parameters were studied, namely types of extractants with their molarity, liquid-to-solid ratio (L/S), temperature and duration. Inorganic acids, including H₂SO₄, HNO₃ and HCl were used to investigate its extraction efficiency on Ca and Al. In this context, HNO₃ was proven to be the best extractant in extracting the Ca, while H₂SO₄ in removing Al. Although H₂SO₄ possessed the highest efficiency in removing Al, deposition of CaSO₄ precipitates on the sludge surface was believed to affect the mass transfer process and ultimately impede the leaching

rate in the subsequent studies. Therefore, HNO₃ was selected as the extractant. In terms of acid concentration, 1.0 M of acid was found to be the most effective.

With the use of 1.0 M HNO₃, L/S ratio of 10:1 achieved the highest efficiency. On top of that, it was observed that there was a positive relationship between the leaching efficiency and the increase of temperature with optimal at 90 °C. The optimum leaching duration was found to be 90 minutes. Overall, the optimal conditions for leaching Al and Ca from the rubber sludge were under 1.0 M of HNO₃, L/S ratio of 10:1, with the temperature of 90 °C and the duration of 90 minutes. The extraction efficiency of Al achieved 100 %, while Ca reached 95.21 %. The post-leached residues further proved the precipitation of CaSO₄ on the sludge surface that leached with H₂SO₄ through the analysis of SEM, XRD, FTIR as well as its physical appearance. Meanwhile, residues from the optimal result demonstrated a more porous structure, rich in carbon content, suggesting its reusability as a low-cost adsorbent, energy source or soil conditioner.

5.2 Recommendations for Future Work

The steps were taken in order to fulfil the project's goals. Several studies have not been thoroughly examined because of unforeseen circumstances, such as deviations from the outcomes that led to repeated experiment work. Therefore, several recommendations are made for future work.

- i. To obtain a more precise measure of the total metal content in the sludge, the acid digestion procedure can be carried out using the microwave digestion method. This can lead to highly reliable extraction efficiency results.
- ii. The leaching agents such as organic acid or alkali can be employed to have an in-depth knowledge on the effect of different leaching agent.
- iii. The leachate sample must be analyzed as soon as possible to avoid degradation.
- iv. The interaction between the parameters can be evaluated through Design of Experiments method to optimize the leaching efficiency.

- v. The rate-controlling step in leaching process can be determined through studying the leaching kinetic.
- vi. Brunauer-Emmett-Telle study, as well as the content of the organic elements can be examined for post-residues sludge to ascertain its reusability.
- vii. The investigation into effective methods for recovering high-purity calcium and aluminum in the form of nitrate crystals can be conducted.
- viii. The post-leached sludge residues can be subjected to pyrolysis process to examine the yield of bio-oil.

REFERENCES

- Abdulatif Mansur, Muthu Pannirselvam, Khalid Al-Hothaly, Eric Adetuty and Andrew Ball, 2015. Recovery and Characterization of Oil from Waste Crude Oil Tank Bottom Sludge from Azzawiya Oil Refinery in Libya. *Journal of Advanced Chemical Engineering*, 05(01).
- Academy of Sciences Malaysia, 2015. *Study on the Current Issues and Needs for Water Supply and Wastewater Management in Malaysia*.
- Agus Mirwan, Susianto Susianto, Ali Altway and Renanto Handogo, 2020. Temperature-dependent Kinetics of Aluminum Leaching from Peat Clay Article History. *Malaysian Journal of Fundamental and Applied Sciences*, 16(2), pp.248–251.
- Ali Fazli and Rodrigue, D., 2020. Waste Rubber Recycling: A Review on the Evolution and Properties of Thermoplastic Elastomers. *Materials*, 13(3).
- Alkan, G., Yagmurlu, B., Cakmakoglu, S., Hertel, T., Kaya, Ş., Gronen, L., Stopic, S. and Friedrich, B., 2018. Novel Approach for Enhanced Scandium and Titanium Leaching Efficiency from Bauxite Residue with Suppressed Silica Gel Formation. *Scientific Reports*, 8(1).
- Amdur, S., 2019. *Latex Compositions and Antistatic Articles Manufactured Therefrom*. US 10,479,874.
- Amin, Z. and Salihoğlu, N.K., 2021. Evaluation of Free Water Removal from Different Sludge by Solar Energy Utilization. *Environmental Engineering Research*, 26(3).
- Anjum, M., Al-Makishah, N.H. and Barakat, M.A., 2016. Wastewater Sludge Stabilization using Pre-treatment Methods. *Process Safety and Environmental Protection*, 102, pp.615–632.
- Aoudia, K., Azem, S., Aït Hocine, N., Gratton, M., Pettarin, V. and Seghar, S., 2017. Recycling of Waste Tire Rubber: Microwave Devulcanization and Incorporation in a Thermoset Resin. *Waste Management*, 60, pp.471–481.
- Appels, L., Baeyens, J., Degreève, J. and Dewil, R., 2008. Principles and Potential of the Anaerobic Digestion of Waste-Activated Sludge. *Progress in Energy and Combustion Science*, 34(6), pp.755–781.
- Arif Billah, Kuaanan Techato and Wirach Taweepreda, 2020. Energy Conversion from Wastewater Sewage Sludge. *Asia-Pacific Journal of Chemical Engineering*, 15(5).
- Awab, H., Paramalinggam, P.T.T. and Mohd Yusoff, A.R., 2012. Characterization of Alum Sludge for Reuse and Disposal. *Malaysian Journal of Fundamental and Applied Sciences*, 8(4).

Awale, R.J., Ali, F.B., Azmi, A.S., Puad, N.I.M., Anuar, H. and Hassan, A., 2018. Enhanced Flexibility of Biodegradable Polylactic Acid/Starch Blends using Epoxidized Palm Oil as Plasticizer. *Polymers*, 10(9).

Azdarpour, A., Asadullah, M., Junin, R., Mohammadian, E., Hamidi, H., Daud, A.R.M. and Manan, M., 2015. Extraction of Calcium from Red Gypsum for Calcium Carbonate Production. *Fuel Processing Technology*, 130(C), pp.12–19.

Aziz, S.Q. and Mustafa, J., 2022. Wastewater Sludge Characteristics, Treatment Techniques and Energy Production. *Reciklaza i održivi razvoj*, 15(1), pp.9–26.

AZO Materials, 2018. *How Does EDX Analysis with a Scanning Electron Microscope (SEM) Work?* [online] Available at: <<https://www.azom.com/article.aspx?ArticleID=16256>> [Accessed 26 July 2023].

Bernard, S. and Gray, N.F., 2000. Aerobic Digestion of Pharmaceutical and Domestic Wastewater Sludges at Ambient Temperature. *Pergamon*, 34(3), pp.725–734.

Bisht, K. and Ramana, P. V., 2017. Evaluation of Mechanical and Durability Properties of Crumb Rubber Concrete. *Construction and Building Materials*, 155, pp.811–817.

Campos, T., Chaer, G., dos Santos Leles, P., Silva, M. and Santos, F., 2019. Leaching of Heavy Metals in Soils Conditioned with Biosolids from Sewage Sludge. *Floresta e Ambiente*, 26(1).

Cao, S., Zhou, C., Pan, J., Liu, C., Tang, M., Ji, W., Hu, T. and Zhang, N., 2018. Study on Influence Factors of Leaching of Rare Earth Elements from Coal Fly Ash. *Energy and Fuels*, 32(7), pp.8000–8005.

Chen, G., Yue, P.L. and Mujumdar, A.S., 2002. Sludge Dewatering and Drying. *Drying Technology*, 20(4–5), pp.883–916.

Chen, H.X., Ma, X. and Dai, H.J., 2010. Reuse of Water Purification Sludge as Raw Material in Cement Production. *Cement and Concrete Composites*, 32(6), pp.436–439.

Chi, R., Tian, J., Zhu, G., Wu, Y., Li, S., Wang, C. and Zhou, Z.A., 2006b. Kinetics of Rare Earth Leaching from a Manganese-Removed Weathered Rare-Earth Mud in Hydrochloric Acid Solutions. *Separation Science and Technology*, 41(6), pp.1099–1113.

Czechowska-Kosacka, A., 2019. Application of Sewage Sludge for the Production of Construction. *MATEC Web of Conferences*, 252, p.05025.

Daeid, N.N., 2005. FORENSIC SCIENCES | Systematic Drug Identification. In: *Encyclopedia of Analytical Science*. Elsevier. pp.471–480.

- Dana Abouelnasr and Isam Zubaidi, 2008. Treatment and Recovery of Oil-based Sludge using Solvent Extraction. *Society of Petroleum Engineers - 13th Abu Dhabi International Petroleum Exhibition and Conference, ADIPEC 2008*, 3, pp.1528–1534.
- Dentel, S.K. and Qi, Y., 2013. 3.12 Management of Sludges, Biosolids, and Residuals. In: *Comprehensive Water Quality and Purification*. Elsevier. pp.223–243.
- Department of Environment, 2022. *Environmental Quality Report 2022*. [online] Available at: <<https://enviro2.doe.gov.my/ekmc/wp-content/uploads/2023/09/Laporan-Kualiti-Alam-Sekeliling-EQR-2022-1.pdf>> [Accessed 26 January 2024].
- Devaraj, V., 2021. *Green Technology to Purify Treated Wastewater and Harvested Rainwater as Process Water for Raw Rubber Processing and Rubber Products Manufacturing*. [online] Available at: <<https://www.myrubbercouncil.com/specialfund/documents/sharing/EP%20Water.pdf>> [Accessed 26 January 2024].
- Devaraj, V., Zairossani, M.N. and Pretibaa, S., 2006. Membrane Separation as a Cleaner Processing Technology for Natural Raw Rubber Processing. *Journal Applied Membrane Science & Technology*, 4, pp.13–22.
- Devi, P. and Saroha, A.K., 2017. Utilization of Sludge Based Adsorbents for the Removal of Various Pollutants: A Review. *Science of the Total Environment*, 578, pp.16–33.
- Domínguez, A., Menéndez, J.A., Inguanzo, M. and Pís, J.J., 2006. Production of Bio-Fuels by High Temperature Pyrolysis of Sewage Sludge using Conventional and Microwave Heating. *Bioresource Technology*, 97(10), pp.1185–1193.
- Egüven, D. and Akinci, G., 2011. Comparison of Acid Digestion Techniques to Determine Heavy Metals in Sediment and Soil Samples. *Gazi University Journal of Science GU J Sci*, 24(1), pp.29–34.
- Elisabeth, M., Terry, M. and Azad, M., 2017. Optimization of An Acid Digestion Procedure for the Determination of Hg, As, Sb, Pb and Cd in Fish Muscle Tissue. *MethodsX*, 4, pp.513–523.
- Emilia Agustina, T., Jefri Sirait, E. and Silalahi, H., 2017. Treatment of Rubber Industry Wastewater by Using Fenton Reagent and Activated Carbon. *Jurnal Teknologi*, 79(7–2), pp.31–37.
- Fernández-Carrasco, L., Torrens-Martín, D., Morales, L.M. and Martínez-Ramírez, S., 2012. Infrared Spectroscopy – Materials Science, Engineering and Technology. *Infrared Spectroscopy in the Analysis of Building and Construction Materials*. [online] Available at: <www.intechopen.com>. [Accessed 28 July 2023].

- Gamaralalage, D., Sawai, O. and Nunoura, T., 2016. Effectiveness of Available Wastewater Treatment Facilities in Rubber Production Industries in Sri Lanka. *International Journal of Environment Science and Development*, 7(12), pp.940–945.
- Gaudino, S., Galas, C., Belli, M., Barbizzi, S., De Zorzi, P., Jaćimović, R., Jeran, Z., Pati, A. and Sansone, U., 2007. The Role of Different Soil Sample Digestion Methods on Trace Elements Analysis: A Comparison of ICP-MS and INAA Measurement Results. *Accreditation and Quality Assurance*, 12(2), pp.84–93.
- Geng, H., Xu, Y., Zheng, L., Gong, H., Dai, L. and Dai, X., 2020. An Overview of Removing Heavy Metals from Sewage Sludge: Achievements and Perspectives. *Environmental Pollution*, 266.
- Ginisty, P., Guei, F., Girault, R., Tosoni, J., Olivier, J. and Vaxelaire, J., 2016. Hal Open Science. *Dryness Limit: A Useful Parameter to Assess Sludge Dewatering*. [online] Available at: <<https://hal.science/hal-01294465>> [Accessed 28 July 2023].
- Gotame, R.C., 2021. Physics Feed. *XRD Working and Application*. [online] Available at: <<https://physicsfeed.com/post/xrd-working-and-application/>> [Accessed 28 July 2023].
- Grobelak, A., Czerwińska, K. and Murtaś, A., 2019. General Considerations on Sludge Disposal, Industrial and Municipal Sludge. In: *Industrial and Municipal Sludge: Emerging Concerns and Scope for Resource Recovery*. Elsevier. pp.135–153.
- Gross, T.S.C., 1993. Thermal Drying of Sewage Sludge. *Water and Environment Journal*, 7(3).
- Guan, Q., Sui, Y., Liu, C., Wang, Y., Zeng, C., Yu, W., Gao, Z., Zang, Z. and Chi, R.A., 2022. Characterization and Leaching Kinetics of Rare Earth Elements from Phosphogypsum in Hydrochloric Acid. *Minerals* 2022, 12(6).
- Gunarathne, V., Rajapaksha, A.U., Vithanage, M., Alessi, D.S., Selvasembian, R., Naushad, M., You, S., Oleszczuk, P. and Ok, Y.S., 2022. Hydrometallurgical Processes for Heavy Metals Recovery from Industrial Sludges. *Critical Reviews in Environmental Science and Technology*, 52(6), pp.1022–1062.
- Gunasekaran, S., Natarajan, R.K. and Kala, A., 2007. FTIR Spectra and Mechanical Strength Analysis of Some Selected Rubber Derivatives. *Spectrochimica Acta - Part A: Molecular and Biomolecular Spectroscopy*, 68(2), pp.323–330.
- Hasyimah Rosman, Aznah Anuar, Inawati Othman, Hasnida Harun, Zuhdi Sulong, Siti Hanna Elias, Mohd Arif Hakimi Mat Hassan, Shreesivadas Chelliapan and Zaini Ujang, 2013. Cultivation of Aerobic Granular Sludge for Rubber Wastewater Treatment. *Bioresource Technology*, 129, pp.620–623.

Havlik, T., Miskufova, A., Turek, P. and Kobialkova, I.U., 2019. Considering the Influence of Calcium on EAF Dust Acid Leaching. *Physicochemical Problems of Mineral Processing*, 55(2), pp.528–536.

Haworth, B., Chadwick, D., Chen, L. and Ang, Y.J., 2018. Thermoplastic Composite Beam Structures from Mixtures of Recycled HDPE and Rubber Crumb for Acoustic Energy Absorption. *Journal of Thermoplastic Composite Materials*, 31(1), pp.119–142.

Haynes, R.J. and Zhou, Y.F., 2015. Use of Alum Water Treatment Sludge to Stabilize C and Immobilize P and Metals in Composts. *Environmental Science and Pollution Research*, 22(18), pp.13903–13914.

He, Q., Qiu, J., Rao, M. and Xiao, Y., 2021. Leaching Behaviors of Calcium and Aluminum from An Ionic Type Rare Earth Ore using MgSO₄ as Leaching Agent. *Minerals*, 11(7).

Homkhiew, C., Boonchouytan, W., Cheewawuttipong, W. and Ratanawilai, T., 2018. Potential Utilization of Rubberwood Flour and Sludge Waste from Natural Rubber Manufacturing Process as Reinforcement in Plastic Composites. *Journal of Material Cycles and Waste Management*, 20(3), pp.1792–1803.

Hosseini, S.A., Raygan, S., Rezaei, A. and Jafari, A., 2017. Leaching of Nickel from a Secondary Source by Sulfuric Acid. *Journal of Environmental Chemical Engineering*, 5(4), pp.3922–3929.

Hou, H., Shao, S., Ma, B., Li, X., Shi, S., Chen, Y. and Wang, C., 2022. Sustainable Process for Valuable-Metal Recovery from Circulating Fluidized Bed Fly Ash through Nitric Acid Pressure Leaching. *Journal of Cleaner Production*, 360, pp. 1–12.

Hu, G., Li, J. and Hou, H., 2015. A Combination of Solvent Extraction and Freeze Thaw for Oil Recovery from Petroleum Refinery Wastewater Treatment Pond Sludge. *Journal of Hazardous Materials*, 283, pp.832–840.

Hu, Z. and Qi, L., 2013. Sample Digestion Methods. In: *Treatise on Geochemistry: Second Edition*. Elsevier Inc. pp.87–109.

Hui, K., Tang, J., Lu, H., Xi, B., Qu, C. and Li, J., 2020. Status and Prospect of Oil Recovery from Oily Sludge: A Review. *Arabian Journal of Chemistry*, 13(8), pp.6523–6543.

Indah Water, 2019. *Sludge Treatment*. [online] Available at: <<http://aozhouiwk.com/sludge-treatment.html>> [Accessed 12 July 2023].

Jing, X., 2004. *Sample Preparation and Heavy Metal Determination by Atomic Spectrometry*. Master of Science. Brock University. Available at: <https://dr.library.brocku.ca/bitstream/handle/10464/1649/Brock_Xiao_Jing_2004.pdf;jsessionid=B869C3C2E86F4184990D035B39891485?sequence=1> [Accessed 31 January 2024].

- Kakubo, T., Matsuura, A., Kawahara, S. and Tanaka, Y., 1998. Origin of Characteristic Properties of Natural Rubber - Effect of Fatty Acids on Crystallization of cis-1,4-polyisoprene. *Rubber Chemistry and Technology*, 71(1), pp.70–75.
- Kamaraj, C., Lakshmi, S., Rose, C. and Muralidharan, C., 2017. Wet Blue Fiber and Lime from Leather Industry Solid Waste as Stabilizing Additive and Filler in Design of Stone Matrix Asphalt. *Asian Journal of Research in Social Sciences and Humanities*, 7(11), pp.240–257.
- Kamizela, T. and Kowalczyk, M., 2019. Sludge dewatering: Processes for enhanced performance. In: *Industrial and Municipal Sludge: Emerging Concerns and Scope for Resource Recovery*. Elsevier. pp.399–423.
- Khoo, D., 2023. Supply of Gloves Continues to Outstrip Demand. *TheStar*, [online] 1 April. Available at: <<https://www.thestar.com.my/business/business-news/2023/04/01/supply-of-gloves-continues-to-outstrip-demand>> [Accessed 26 January 2024].
- Kuan, Y.C., Lee, I.H. and Chern, J.M., 2010. Heavy Metal Extraction from PCB Wastewater Treatment Sludge by Sulfuric Acid. *Journal of Hazardous Materials*, 177(1–3), pp.881–886.
- Kurniawan, M.R., Imami, T.G., Ichlas, Z.T., Hidayat, T. and Mubarok, M.Z., 2022. Production of Synthetic Rutile from Tin Ore Beneficiation Byproduct through Preoxidation and Reductive Leaching in Hydrochloric Acid. *Scientific Reports*, 12(1).
- Kurniawati, D., Aziz, H., Chaidir, Z. and Zein, R., 2018. Removal of Zinc onto Several Adsorbents Derived from Waste Activated Sludge of Crumb Rubber Industry (CRI-WAS). *Advanced Science Engineering Information Technology*, 8(1), pp.157–164.
- Lamastra, L., Suci, N.A. and Trevisan, M., 2018. Sewage Sludge for Sustainable Agriculture: Contaminants' Contents and Potential Use as Fertilizer. *Chemical and Biological Technologies in Agriculture*, 5(1).
- Latif Ahmad, A., Ibrahim, N., Ismail, S. and Bhatia, S., 2002. Coagulation-Sedimentation-Extraction Pretreatment Methods for the Removal of Suspended Solids and Residual Oil from Palm Oil Mill Effluent (POME). *IJUM Engineering Journal*, 3(1).
- Laura Martín-Pozo, María del Carmen Gómez-Regalado, María Teresa García-Córcoles and Alberto Zafra-Gómez, 2022. Chapter 16 - Removal of Quinolone Antibiotics from Wastewaters and Sewage Sludge. In: *Emerging Contaminants in the Environment*, Elsevier. Candice Janco. pp.381–406.
- Lee, Y.H., Eom, H., Lee, S.M. and Kim, S.S., 2021. Effects of pH and Metal Composition on Selective Extraction of Calcium from Steel Slag for Ca(OH)₂ Production. *RSC Advances*, 11(14), pp.8306–8313.

Lo, K.S.L. and Chen, Y.H., 1990. Extracting Heavy Metals from Municipal and Industrial Sludges. *The Science of the Total Environment*, 90, pp.99–116.

Lovato, M.J., del Valle, L.J., Puiggali, J. and Franco, L., 2023. Performance-Enhancing Materials in Medical Gloves. *Journal of Functional Biomaterials*, 14(7), pp.1–34.

Massoudinejad, M., Mehdipour-Rabori, M. and Dehghani, M.H., 2015. Treatment of Natural Rubber Industry Wastewater through a Combination of Physicochemical and Ozonation Processes. *J Adv Environ Health Res*, 3(4), pp.242–251.

Matusiewicz, H., 2003. Wet Digestion Methods. *Comprehensive Analytical Chemistry 41*. pp.193–233.

measurlabs, 2023. *SEM-EDX Analysis*. [online] Available at: <<https://measurlabs.com/methods/scanning-electron-microscopy-x-ray-spectroscopy-sem-edx/>> [Accessed 26 July 2023].

Michalak, I., Marycz, K., Basińska, K. and Chojnacka, K., 2014. Using SEM-EDX and ICP-OES to Investigate the Elemental Composition of Green Macroalga *Vaucheria Sessilis*. *Scientific World Journal*, 2014, 891928.

Mingot, J.I., Obrador, A., Manuel Alvarez, J. and Rico, M.I., 1995. Acid Extraction and Sequential Fractionation of Heavy Metals in Water Treatment Sludges. *Environmental Technology (United Kingdom)*, 16(9), pp.869–876.

Mirwan, A., Susianto, Altway, A. and Handogo, R., 2017. A modified shrinking core model for leaching of aluminum from sludge solid waste of drinking water treatment. *International Journal of Technology*, 8(1), pp.19–26.

Molla, M.R., Begum, M.H.A., Farhad, S.F.U., Asadur Rahman, A.S.M., Tanvir, N.I., Bashar, M.S., Bhuiyan, R.H., Alam, M.S., Hossain, M.S. and Rahman, M.T., 2022. Facile Extraction and Characterization of Calcium Hydroxide from Paper Mill Waste Sludge of Bangladesh. *Royal Society Open Science*, 9(8), pp.1–11.

Nadesan, S.M., Sibelco Nederland NV. 2018. *Nitrile Rubber Products and Methods of Forming Nitrile Rubber Products*. Malaysia. WO2018099674A1.

Naoum, C., Fatta, D., Haralambous, K.J. and Loizidou, M., 2001. Removal of heavy metals from sewage sludge by acid treatment. *Journal of Environmental Science and Health - Part A Toxic/Hazardous Substances and Environmental Engineering*, 36(5), pp.873–881.

Nayak, N. and Panda, C.R., 2010. Aluminium Extraction and Leaching Characteristics of Talcher Thermal Power Station Fly Ash with Sulphuric Acid. *Fuel*, 89(1), pp.53–58.

Nezhdbahadori, F., Abdoli, M.A., Baghdadi, M. and Ghazban, F., 2018. A Comparative Study on the Efficiency of Polar and Non-polar Solvents in Oil

- Sludge Recovery using Solvent Extraction. *Environmental Monitoring and Assessment*, 190(7).
- Ng, H.M., Saidi, N.M., Omar, F.S., Ramesh, K., Ramesh, S. and Bashir, S., 2018. Thermogravimetric Analysis of Polymers. In: *Encyclopedia of Polymer Science and Technology*. John Wiley & Sons, Inc. pp.1–29.
- Nicoara, A.I., Voineagu, T.G., Alecu, A.E., Vasile, B.S., Maior, I., Cojocaru, A., Trusca, R. and Popescu, R.C., 2023. Fabrication and Characterisation of Calcium Sulphate Hemihydrate Enhanced with Zn- or B-Doped Hydroxyapatite Nanoparticles for Hard Tissue Restoration. *Nanomaterials*, 13(15).
- Nielsen, S. and Stefanakis, A.I., 2020. Sustainable Dewatering of Industrial Sludges in Sludge Treatment Reed Beds: Experiences from Pilot and Full-scale Studies under Different Climates. *Applied Sciences*, 10(21), pp.1–21.
- Noorain, R., 2013. Study on the Characteristics and Utilization of Sewage Sludge at Indah Water Konsortium (IWK) Sungai Udang, Melaka. *International Journal of Environmental and Ecological Engineering*, 7(8), pp.544–548.
- Onchoke, K.K., Franclemont, C.M. and Weatherford, P.W., 2018. Structural Characterization and Evaluation of Municipal Wastewater Sludge (biosolids) from Two Rural Wastewater Treatment Plants in East Texas, USA. *Spectrochimica Acta - Part A: Molecular and Biomolecular Spectroscopy*, 204, pp.514–524.
- Partridge, J.A. and Bosuego, G.P., 1980. *Acid Digestion of Organic Liquids*. [online] United States of America. Available at: <<https://www.osti.gov/servlets/purl/6921445>> [Accessed 31 January 2024].
- Perapong, T. and Surajit, T., 2006. Environmental Problems Related to Natural Rubber Production in Thailand. *Feature Article*, 21(2), pp.122–129.
- Perrella, F.W. and Gaspari, A.A., 2002. Natural Rubber Latex Protein Reduction with an Emphasis on Enzyme Treatment. *Methods*, 27(1), pp.77–86.
- Qrenawi, L.I. and Rabah, F.K.J., 2021. Sludge Management in Water Treatment Plants: Literature Review. *International Journal of Environment and Waste Management*, 27(1), pp.93–125.
- Rahmah, M., Ahmad Khusyairi, A.R., Nur Khairunnisya, H. and Siti Nurbalqis, M., 2019. Oven Ageing versus UV Ageing Properties of Natural Rubber Cup Lump/EPDM Rubber Blend with Mangosteen Powder (MPP) as Natural Antioxidant. In: *IOP Conference Series: Materials Science and Engineering*. Institute of Physics Publishing. pp.1–12.
- Rakotonimaro, T. V., Neculita, C.M., Bussière, B., Benzaazoua, M. and Zagury, G.J., 2017. Recovery and Reuse of Sludge from Active and Passive Treatment of Mine Drainage-impacted Waters: A Review. *Environmental Science and Pollution Research*, 24(1), pp.73–91.

- Ramanathan, T. and Ting, Y.-P., 2015. Selection of Wet Digestion Methods for Metal Quantification in Hazardous Solid Wastes. *Journal of Environmental Chemical Engineering*, 3(3), pp.1459–1467.
- Rani, A., Rashid, N.A., Abdullah, M.A.H. and Omar, M.F., 2020. Evaluation on Physical and Chemical Properties of Treated Industrial Wastewater Sludge Containing Latex and Heavy Metals using Ordinary Portland Cement via Stabilization / Solidification Technique. In: *IOP Conference Series: Materials Science and Engineering*. IOP Publishing Ltd.
- Rincón, J., Cañizares, P. and García, M.T., 2005. Regeneration of Used Lubricant Oil by Polar Solvent Extraction. *Industrial and Engineering Chemistry Research*, 44(12), pp.4373–4379.
- Rolere, S., Liengprayoon, S., Vaysse, L., Sainte-Beuve, J. and Bonfils, F., 2015. Investigating Natural Rubber Composition with Fourier Transform Infrared (FT-IR) Spectroscopy: A Rapid and Non-destructive Method to Determine Both Protein and Lipid Contents Simultaneously. *Polymer Testing*, 43, pp.83–93.
- Rorat, A., Courtois, P., Vandenbulcke, F. and Lemiere, S., 2019. Sanitary and Environmental Aspects of Sewage Sludge Management. In: *Industrial and Municipal Sludge: Emerging Concerns and Scope for Resource Recovery*. Elsevier. pp.155–180.
- Roychand, R., Gravina, R.J., Zhuge, Y., Ma, X., Mills, J.E. and Youssf, O., 2021. Practical Rubber Pre-treatment Approach for Concrete Use—An Experimental Study. *Journal of Composites Science*, 5(6), 143.
- Safeer Abbas, Ali Ahmed, Ayesha Waheed, Wasim Abbass, Muhammad Yousaf, Sbahat Shaukat, Hisham Alabduljabbar and Youssef Ahmed Awad, 2022. Recycled Untreated Rubber Waste for Controlling the Alkali–Silica Reaction in Concrete. *Materials*, 15(10).
- Santos, M.T. and Lopes, P.A., 2022. Sludge Recovery from Industrial Wastewater Treatment. *Sustainable Chemistry and Pharmacy*, 29.
- Sastre, J., Sahuquillo, A., Vidal, M. and Rauret, G., 2002. Determination of Cd, Cu, Pb and Zn in Environmental Samples: Microwave-assisted Total Digestion Versus Aqua Regia and Nitric Acid Extraction. *Analytica Chimica Acta*, 462(1), pp.59–72.
- Shamaki, M., Adu-Amankwah, S. and Black, L., 2021. Reuse of UK Alum Water Treatment Sludge in Cement-Based Materials. *Construction and Building Materials*, 275.
- Silva, N.G.S., Cortat, L.I.C.O., Orlando, D. and Mulinari, D.R., 2020. Evaluation of Rubber Powder Waste as Reinforcement of the Polyurethane Derived from Castor Oil. *Waste Management*, 116, pp.131–139.

- Smith, K.M., Fowler, G.D., Pullket, S. and Graham, N.J.D., 2009. *Sewage Sludge-based Adsorbents: A Review of Their Production, Properties and Use in Water Treatment Applications*. *Water Research*.
- Soliman, N.K. and Moustafa, A.F., 2020. Industrial Solid Waste for Heavy Metals Adsorption Features and Challenges; A Review. *Journal of Materials Research and Technology*, 9(5), pp.10235–10253.
- Stylianou, M.A., Kollia, D., Haralambous, K.J., Inglezakis, V.J., Moustakas, K.G. and Loizidou, M.D., 2007. Effect of Acid Treatment on the Removal of Heavy Metals from Sewage Sludge. *Desalination*, 215(1–3), pp.73–81.
- Su, R., Liang, B. and Guan, J., 2016. Leaching Effects of Metal from Electroplating Sludge under Phosphate Participation in Hydrochloric Acid Medium. *Procedia Environmental Sciences*, 31, pp.361–365.
- Supaporn, P., Ly, H.V., Kim, S.S. and Yeom, S.H., 2019. Bio-oil Production using Residual Sewage Sludge After Lipid and Carbohydrate Extraction. *Environmental Engineering Research*, 24(2), pp.202–210.
- Taiwo, E.A. and Otolorin, J.A., 2009. Oil Recovery from Petroleum Sludge by Solvent Extraction. *Petroleum Science and Technology*, 27(8), pp.836–844.
- Tao, L., Wang, L., Yang, K., Wang, X., Chen, L. and Ning, P., 2021. Leaching of Iron from Copper Tailings by Sulfuric Acid: Behavior, Kinetics and Mechanism. *RSC Advances*, 11(10), pp.5741–5752.
- Tertyshnaya, Y. V., Karpova, S.G., Podzorova, M. V., Khvatov, A. V. and Moskovskiy, M.N., 2022. Thermal Properties and Dynamic Characteristics of Electrospun Polylactide/Natural Rubber Fibers during Disintegration in Soil. *Polymers*, 14(5).
- Thong, O., Ibrahim, A., Abdul Rahim, H., Yong, W.J. and Ismail, N., 2021. Review of Crude Oil Extraction Methods from Petroleum Sludge. *International Journal of Engineering Technology and Sciences*, 8(1), pp.40–50.
- Twyman, R.M., 2005. Sample Dissolution for Elemental Analysis: Wet Digestion. In: P. Worsfold, A. Townshend and C. Poole, eds. *Encyclopedia of Analytical Science*, Second. Elsevier. pp.146–153.
- Uddin, A.H., Khalid, R.S., Alaama, M., Abdualkader, A.M., Kasmuri, A. and Abbas, S.A., 2016. Comparative Study of Three Digestion Methods for Elemental Analysis in Traditional Medicine Products using Atomic Absorption Spectrometry. *Journal of Analytical Science and Technology*, 7(1).
- Uttara Mahapatra, Abhijit Chatterjee, Chandan Das and Ajay Kumar Manna, 2021. Adsorptive Removal of Hexavalent Chromium and Methylene Blue from Simulated Solution by Activated Carbon Synthesized from Natural Rubber Industry Biosludge. *Environmental Technology and Innovation*, 22.
- Uttara Mahapatra, Ajay Kumar Manna and Abhijit Chatterjee, 2022. A Critical Evaluation of Conventional Kinetic and Isotherm Modeling for Adsorptive

Removal of Hexavalent Chromium and Methylene Blue by Natural Rubber Sludge-derived Activated Carbon and Commercial Activated Carbon. *Bioresource Technology*, 343.

Valera-Zaragoza, M., Yescas-Yescas, A., Juarez-Arellano, E.A., Aguirre-Cruz, A., Aparicio-Saguilán, A., Ramírez-Vargas, E., Sepúlveda-Guzmán, S. and Sánchez-Valdes, S., 2014. Immobilization of TiO₂ Nanoparticles on Montmorillonite Clay and Its Effect on the Morphology of Natural Rubber Nanocomposites. *Polymer Bulletin*, 71(6), pp.1295–1313.

Veeken, A.H.M. and Hamelers, H.V.M., 1999. Removal of Heavy Metals from Sewage Sludge by Extraction with Organic Acids. *Water Science and Technology*, 40(1), pp.129–136.

Veerasingam, S. and Venkatachalapathy, R., 2014. Estimation of Carbonate Concentration and Characterization of Marine Sediments by Fourier Transform Infrared Spectroscopy. *Infrared Physics and Technology*, 66, pp.136–140.

Wahab, Deniyatno, Marthines Sarangas and Yayat Supriyatna, 2021. Kinetics Study of Leaching Ore Nickel Laterite using Hydrochloric Acid in Atmosphere Pressure. *Indonesian Journal of Geology and Mining*, 32(1), pp.14–26.

Wang, G.R., Liu, Y.Y., Tong, L.L., JIN, Z.N., Chen, G. bao and Yang, H.Y., 2019. Effect of Temperature on Leaching Behavior of Copper Minerals with Different Occurrence States in Complex Copper Oxide Ores. *Transactions of Nonferrous Metals Society of China (English Edition)*, 29(10), pp.2192–2201.

Wang, L., Song, S., Gao, H., Wang, L., Yang, S. and Liu, C., 2020. The Optimization and Characterization of the Recycling Utilization of Raffinate in the Copper Leaching Process. *Journal of Materials Research and Technology*, 9(2), pp.2214–2222.

Water Services Industry Act, 2006. *Law of Malaysia Act 655*.

Watkins, P.S., Castellon, B.T., Tseng, C., Wright, M. V., Matson, C.W. and Cobb, G.P., 2018. Validation of a Sulfuric Acid Digestion Method for Inductively Coupled Plasma Mass Spectrometry Quantification of TiO₂ Nanoparticles. *Bulletin of Environmental Contamination and Toxicology*, 100(6), pp.809–814.

Widi Astuti, Hirajima, T., Sasaki, K. and Okibe, N., 2016. Comparison of Effectiveness of Citric Acid and Other Acids in Leaching of Low-grade Indonesian Saprolitic Ores. *Minerals Engineering*, 85, pp.1–16.

Wijerathna, W.S.M.S.K., Wimalaweera, T.I.P., Samarajeewa, D.R., Lindamulla, L.M.L.K.B., Rathnayake, R.M.L.D., Nanayakkara, K.G.N., Jegatheesan, V., Wei, Y. and Jinadasa, K.B.S.N., 2023. Imperative Assessment on The Current Status of Rubber Wastewater Treatment: Research Development and Future Perspectives. *Chemosphere*, 338.

Wu, C.H., Kuo, C.Y. and Lo, S.L., 2004. Removal of Metals from Industrial Sludge by Extraction with Different Acids. *Journal of Environmental Science and Health*, 39(8), pp.2205–2219.

Xiao, L., Cheng, X., Zhang, T., Guo, M. and Zhang, M., 2022. Efficient Inorganic/Organic Acid Leaching for the Remediation of Protogenetic Lead-Contaminated Soil. *Applied Sciences (Switzerland)*, 12(8).

Yang, J., Zhou, Y., Zhang, Z. liang, Xu, K. hua, Zhang, K., Lai, Y. qing and Jiang, L. xing, 2023. Effect of Electric Field on Leaching Valuable Metals from Spent Lithium-Ion Batteries. *Transactions of Nonferrous Metals Society of China (English Edition)*, 33(2), pp.632–641.

Yang, W., Song, W., Li, J. and Zhang, X., 2020. Bioleaching of Heavy Metals from Wastewater Sludge with the Aim of Land Application. *Chemosphere*, 249.

Yoshizaki, S. and Tomida, T., 2000. Principle and Process of Heavy Metal Removal from Sewage Sludge. *Environmental Science and Technology*, 34(8), pp.1572–1575.

Zhen, G. and Zhao, Y., 2017. Sewage Sludge Generation and Characteristics. In: *Pollution Control and Resource Recovery: Sewage Sludge*. Elsevier. pp.1–11.

Zubaidy, E.A.H. and Abouelnasr, D.M., 2010. Fuel Recovery from Waste Oily Sludge using Solvent Extraction. *Process Safety and Environmental Protection*, 88(5), pp.318–326.

APPENDICES

Appendix A: Preparation for Multi-Element Standard Solution

To prepare a 100-ml of 500 ppm standard solution containing of Ca^{2+} ions and Al^{3+} ions, about 0.295 g of $\text{Ca}(\text{NO}_3)_2 \cdot 4\text{H}_2\text{O}$ and 0.695 g of $\text{Al}(\text{NO}_3)_3 \cdot 9\text{H}_2\text{O}$ as the precursors were used. A sample calculation to determine the amount of salts needed was shown:

Aluminium Nitrate Nonahydrate

500 ppm = 0.5 g/L

Molecular Weight of $\text{Al}(\text{NO}_3)_3 \cdot 9\text{H}_2\text{O}$ = 375.13 g/mol

Molecular Weight of Al = 27 g/mol

There is 1 mol of Al in $\text{Al}(\text{NO}_3)_3 \cdot 9\text{H}_2\text{O}$.

Amount of Al salt required

$$= \frac{0.5 \text{ g Al}}{\text{L solution}} \left(\frac{1 \text{ mol Al}}{27 \text{ g}} \right) \left(\frac{1 \text{ mol Al}(\text{NO}_3)_3 \cdot 9\text{H}_2\text{O}}{1 \text{ mol Al}} \right) \left(\frac{375.13 \text{ g Al}(\text{NO}_3)_3 \cdot 9\text{H}_2\text{O}}{1 \text{ mol}} \right)$$

Amount of Al salt required in 1 L solution = 6.95 g

Amount of Al salt required in 100 ml solution = 0.695 g

Calcium Nitrate Tetrahydrate

500 ppm = 0.5 g/L

Molecular Weight of $\text{Ca}(\text{NO}_3)_2 \cdot 4\text{H}_2\text{O}$ = 236.15 g/mol

Molecular Weight of Ca = 40.08 g/mol

There is 1 mol of Ca in $\text{Ca}(\text{NO}_3)_2 \cdot 4\text{H}_2\text{O}$.

Amount of Ca salt required

$$= \frac{0.5 \text{ g Ca}}{\text{L solution}} \left(\frac{1 \text{ mol Ca}}{40.08 \text{ g}} \right) \left(\frac{1 \text{ mol Ca}(\text{NO}_3)_2 \cdot 4\text{H}_2\text{O}}{1 \text{ mol Ca}} \right) \left(\frac{236.15 \text{ g Ca}(\text{NO}_3)_2 \cdot 4\text{H}_2\text{O}}{1 \text{ mol}} \right)$$

Amount of Ca salt required in 1 L solution = 2.95 g

Amount of Ca salt required in 100 ml solution = 0.295 g

Table A-1: Volume of Multi-Element Standard Solution Required for the Preparation of Various Concentration of Ions in 100 ml Solution.

Concentration of Ions (mg/L)	Volume of Multi-Element Standard Solution (mL)
10	2
20	4
30	6
40	8
50	10

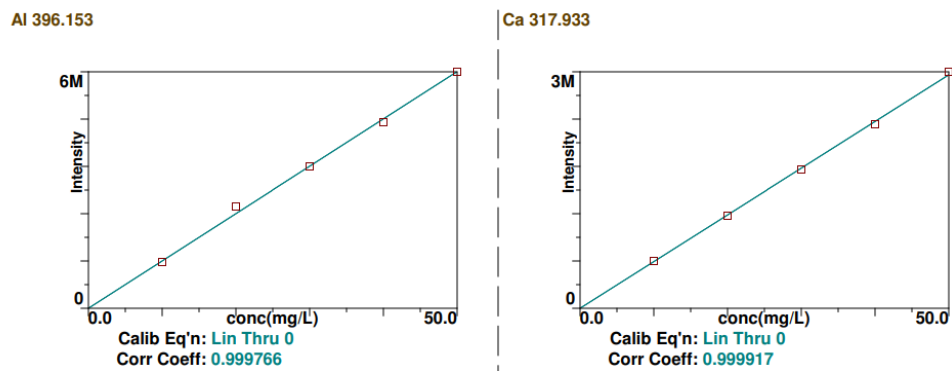
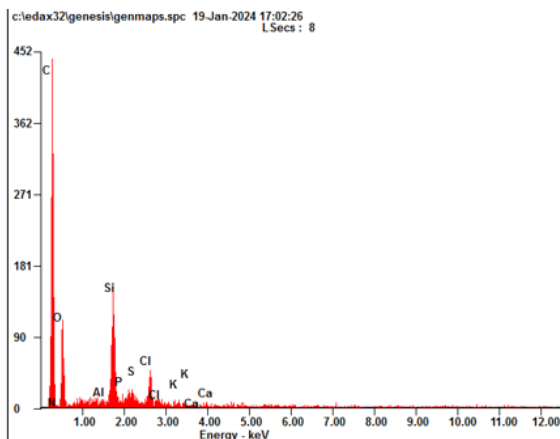


Figure A-1: Calibration Curve of Standard Solution.

Appendix B: EDX Result of Residues from Acid Digestion



<i>Element</i>	<i>Wt%</i>	<i>At%</i>
<i>CK</i>	67.34	75.68
<i>NK</i>	01.91	01.84
<i>OK</i>	21.84	18.43
<i>AlK</i>	00.09	00.04
<i>SiK</i>	06.42	03.08
<i>PK</i>	00.08	00.04
<i>SK</i>	00.14	00.06
<i>ClK</i>	02.11	00.80
<i>KK</i>	00.07	00.02
<i>CaK</i>	00.00	00.00
<i>Matrix</i>	Correction	ZAF

Figure B-1: EDX of Residues from Acid Digestion.

Appendix C: Preparation of Acid for Leaching Process

Molarity of $H_2SO_4 = 17.8 \text{ M}$

Molarity of $HNO_3 = 15.4 \text{ M}$

Molarity of $HCl = 12.08 \text{ M}$

To prepare 50 ml of 1.0 M H_2SO_4

$$M_1V_1 = M_2V_2$$

$$17.8 (V_1) = (1)(50)$$

$$V_1 = 2.8 \text{ ml } H_2SO_4$$

The steps were repeated to calculate 1.0 M of HNO_3 and HCl , as well as 0.3 M and 0.5 M of H_2SO_4 , HNO_3 and HCl .

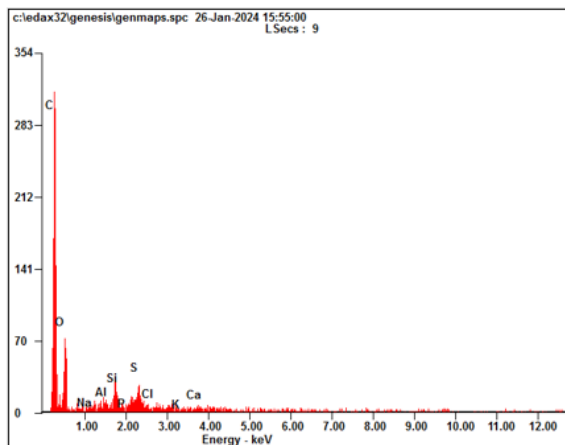
Appendix D: ICP-OES Result Analysis

Table D-1: ICP-OES Result with Its Extraction Efficiency during Leaching Process.

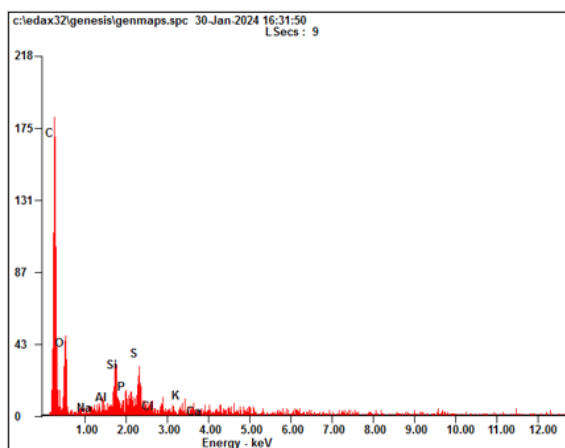
Acid Digestion (3 g sludge : 100 ml Aqua Regia)				
	Element	ICP-OES Result (mg/l)	Leached Content (mg element / g sludge)	Extraction Efficiency
	Al	28.48	47.47	-
	Ca	43.13	71.88	-
Acid Leaching				
Parameter: Acid and Concentration				
0.3 M H₂SO₄	Al	1.173	0.5865	1.24
	Ca	49.31	24.655	34.28
0.5 M H₂SO₄	Al	22.31	22.31	47.00
	Ca	14.33	14.33	19.94
1.0 M H₂SO₄	Al	33.57	33.57	70.72
	Ca	9.031	9.031	12.56
0.3 M HNO₃	Al	0.031	0.0155	0.03
	Ca	93.83	46.915	65.27
0.5 M HNO₃	Al	1.035	1.035	2.18
	Ca	54.18	54.18	75.37
1.0 M HNO₃	Al	24.71	24.71	52.05
	Ca	54.63	56.63	78.78
0.3 M HCl	Al	0.114	0.057	0.12
	Ca	47.96	23.98	33.36
0.5 M HCl	Al	0.264	0.264	0.56
	Ca	43.25	43.25	60.17
1.0 M HCl	Al	28.86	24.05	50.67
	Ca	55.96	46.63	64.87

Table D-1 (Continued)

Parameter: L/S Ratio				
3 :1	Al	1.435	1.435	3.02
	Ca	33.61	56.02	77.93
5 :1	Al	32.65	32.65	68.79
	Ca	32.89	54.82	76.26
10 :1	Al	35.32	35.32	74.41
	Ca	37.80	63.00	87.64
Parameter: Temperature				
30	Al	29.82	29.82	62.82
	Ca	36.69	36.69	51.04
50	Al	30.00	30.00	63.20
	Ca	48.94	48.94	68.08
70	Al	35.91	35.91	75.65
	Ca	61.11	61.11	85.01
90	Al	44.06	44.06	92.82
	Ca	67.67	67.67	94.14
Parameter: Duration				
30	Al	28.66	38.21	80.51
	Ca	28.09	56.18	78.15
60	Al	30.75	41.00	86.38
	Ca	29.92	59.84	83.25
90	Al	37.10	49.47	100
	Ca	34.22	68.44	95.21
120	Al	29.10	38.80	81.74
	Ca	29.55	59.10	82.22

Appendix E: EDX Results of Post-Leached Sludge with HNO₃

<i>Element</i>	<i>Wt%</i>	<i>At%</i>
<i>CK</i>	68.58	76.23
<i>OK</i>	25.00	20.86
<i>NaK</i>	00.48	00.28
<i>AlK</i>	00.48	00.24
<i>SiK</i>	02.59	01.23
<i>PK</i>	00.58	00.25
<i>SK</i>	01.79	00.75
<i>ClK</i>	00.16	00.06
<i>KK</i>	00.12	00.04
<i>CaK</i>	00.23	00.08
<i>Matrix</i>	Correction	ZAF



<i>Element</i>	<i>Wt%</i>	<i>At%</i>
<i>CK</i>	68.14	77.24
<i>OK</i>	21.15	18.00
<i>NaK</i>	00.30	00.18
<i>AlK</i>	00.71	00.36
<i>SiK</i>	03.38	01.64
<i>PK</i>	01.31	00.58
<i>SK</i>	03.27	01.39
<i>ClK</i>	00.69	00.27
<i>KK</i>	00.55	00.19
<i>CaK</i>	00.51	00.17
<i>Matrix</i>	Correction	ZAF

Figure E-1: EDX of Post-Leached Sludge with HNO₃ at Different Locations.